Check for updates

Exploration

REVIEW OPEN ACCESS

Recent Advances in Conjugated Microporous Polymers for Photocatalysis: Mechanism, Synthesis and Applications

Dun Zhou[1] | Kongqing Zhang[1] | Xiaobai Li[1] | Yongpeng Liu[3] | Liang Yao[4] | Hongwei Ma[1,2]

[1]College of Chemistry Chemical Engineering and Resource Utilization, Northeast Forestry University, Harbin, P. R. China | [2]Heilongjiang Key Laboratory of Complex Traits and Protein Machines in Organisms, Northeast Forestry University, Harbin, P. R. China | [3]Yusuf Hamied Department of Chemistry, University of Cambridge, Cambridge, UK | [4]State Key Laboratory of Luminescent Materials and Devices, Institute of Polymer Optoelectronic Materials and Devices, Guangdong Basic Research Center of Excellence for Energy and Information Polymer Materials, South China University of Technology, Guangzhou, P. R. China

Correspondence: Xiaobai Li (lixiaobai2008@126.com) | Yongpeng Liu (yl862@cam.ac.uk) | Liang Yao (liangyao@scut.edu.cn) | Hongwei Ma (mahw@nefu.edu.cn)

Received: 17 December 2024 | **Revised:** 5 September 2025 | **Accepted:** 13 October 2025

Keywords: conjugated microporous polymers | photocatalysts | CO_2 reduction | nanomaterials | solar energy conversion

ABSTRACT

As the global energy crisis intensifies and environmental pollution continues to deteriorate, harnessing solar energy through photocatalytic processes is emerging as a leading strategy to meet energy needs and combat climate crisis. Natural photosynthesis, the oldest and most fundamental photocatalytic system, converts sunlight, water, and CO_2 into useful chemicals that sustain all forms of life. Inspired by this process, a range of artificial photosynthesis systems have been developed to store solar energy in chemical bonds. Conjugated microporous polymers (CMPs) have gained increasing attention as innovative photocatalysts, owing to their unique properties such as tunable light-harvesting abilities, robust porous architectures, and extended π-conjugated frameworks. This review outlines recent progress in the application of CMPs as photocatalysts, offering a comprehensive and critical analysis. It begins by introducing the evolution, preparation methods, and catalytic mechanisms of CMPs. The application of CMP-based photocatalysis in hydrogen evolution, CO_2 conversion, biomass valorization, and degradation of harmful substances are then described. Finally, future perspectives of CMPs as photocatalysts are presented, highlighting the key challenges and opportunities in their adaptation for solar energy conversion.

1 | Introduction

As human civilization progresses, the growing dependence on fossil fuels has driven industrial growth while simultaneously leading to two pressing and interconnected issues—rising energy shortages and worsening climate change—both of which demand urgent and innovative solutions on a global scale [1–3]. In response, there has been a growing commitment to developing renewable energy sources, which offer promising strategies to address these pressing issues [4, 5]. Solar energy is considered the cleanest, most plentiful, and economically viable renewable resource, with the capacity to fulfill worldwide energy needs—provided it can be harnessed and stored efficiently. Natural photosynthesis, refined over millions of years of evolution, serves as an exceptional model for solar energy conversion and storage [6], which employs enzymes for selective catalysis and utilizes complementary light absorption in a Z-scheme architecture [7, 8]. Inspired by this process, researchers have created artificial photosynthetic systems using synthetic materials to mimic and drive these processes [9, 10]. Fujishima and Honda pioneered photoelectrochemical water splitting in their seminal 1972 work, which used a TiO_2 electrode to convert sunlight into chemical energy stored in H_2 and O_2 [11].

This is an open access article under the terms of the Creative Commons Attribution License, which permits use, distribution and reproduction in any medium, provided the original work is properly cited.

© 2025 The Author(s). *Exploration* published by Henan University and John Wiley & Sons Australia, Ltd.

Although inorganic materials have advanced considerably, they still suffer from key limitations, including restricted light absorption, fast recombination of photoinduced charge carriers, and poor utilization of the full solar spectrum [12–16]. To address these limitations, researchers have employed porous materials for photocatalytic synthesis [17], as these materials offer distinct advantages due to their tailored structures. Since their first report in 2007 [18], Conjugated microporous polymers (CMPs) have gained wide attention due to their amorphous microporous structures, remarkable stability, and ease of functional modification. These characteristics have enabled CMPs to find applications in gas storage, light collection materials, chemiluminescence sensing, and heterogeneous catalysis [19, 20]. In addition to their well-known applications, CMPs have recently gained recognition as a powerful platform for driving a variety of photocatalytic chemical reactions. demonstrating significant potential in the field. However, despite these advancements, several challenges must still be addressed to fully harness their capabilities, requiring further investigation: (1) Improving the accessibility of catalytic active sites, (2) design with narrow-bandgap CMPs to enhance light absorption, and (3) achieving precise control over CMPs morphology for optimized photocatalytic performance.

Despite extensive research on CMPs as photocatalysts, recent advancements in the field have not been comprehensively reviewed. A time and thorough evaluation of the progress in CMP-based photocatalysts is therefore warranted. This review summarizes recent advancements in CMPs for photocatalysis, focusing on their underlying mechanisms, synthetic strategies, and diverse applications, including hydrogen evolution reaction, CO_2 conversion, biomass valorization, polymerization reactions, degradation of harmful substances, selective sulfur oxidation, synthesis of benzoheterocyclic compounds, cyanide oxidation of tertiary amines, aryl boronic acid hydroxylation, oxidative coupling of amines and the other reactions. A forward-looking perspective on the key hurdles and promising avenues for the development of CMPs photocatalysts is also provided (Figure 1).

2 | Photocatalytic Mechanism and Preparation Method of CMPs

2.1 | Photocatalytic Mechanism of CMPs

CMPs photocatalysis usually operates via three primary stages (Figure 2): (1) Light absorption: Upon absorbing photons, electrons are excited from the valence band (VB) into the conduction band (CB), producing an energized excited state. (2) Separation and migration of charge carriers: The separated charge carriers, originating within or at the surface of the catalyst, migrate to reactive sites to initiate catalytic activity. (3) Surface catalytic reaction: At the catalytic sites, the generated charge carriers engage with the adsorbed reactant species, driving chemical transformations that yield the intended products [5, 21, 22].

Enhancing the efficiency of photocatalysis remains a primary focus of research, with several strategies being employed to achieve this goal. The main approaches to improving photocatalytic efficiency include: Critical methods such as boosting photon capture [23], enhancing charge transport efficiency [24, 25], and tailoring surface morphology. Numerous methods have also been employed to eliminate these barriers, including elemental doping with nitrogen, oxygen, phosphorus, sulfur, boron, chlorine, and fluorine atoms [26], construction of heterojunctions by combining bandgap energy diversifying materials [27], utilization of donor-acceptor (D–A) structure designs to facilitate electron transfer as well as decrease bandgaps to enable broader light harvesting [28], and utilization of cocatalysts or sacrificial molecules to hinder electron-hole recombination. Additionally, reaction conditions, including light intensity, pH, temperature, and solvent choice, also play a crucial role in enhancing photocatalytic performance.

2.2 | Preparation Methods of CMPs

The structural and functional versatility of CMPs is fundamentally governed by the selection of their constituent monomers and synthetic pathways, which directly determine the topological architecture of the polymer network and ultimately define their resulting molecular functionalities. Typically, CMPs are obtained by reacting different monomer units, or alternatively, through self-condensation of a single monomer. Various coupling techniques (Figure 3) have been established for their construction, including Sonogashira–Hagihara [29–32], Suzuki–Miyaura [33–35], Yamamoto [36], Heck [37], Buchwald–Hartwig [38], oxidative polymerization [39–41], Schiff base condensation [42–44], cyclotrimerization [45], phenazine ring fusion [46], heterocycle linkages formations [47–49], etc. These successful reaction designs have promoted the development of CMPs materials from building block design to synthesis methods, and have also developed CMPs with multiple properties, which together form the foundation of the CMPs edifice. The design, synthesis, and classification of CMPs have been extensively reviewed in recent years [19], therefore, these aspects fall beyond the scope of the current review. Instead, this review primarily focuses on the applications of CMPs photocatalysts.

3 | CMPs-Based Photocatalytic Applications

3.1 | Hydrogen Evolution Reaction (HER)

Photocatalytic water splitting is one promising solution to convert sunlight into clean as well as renewable chemical fuels, which can offer a potential solution to the energy crisis as well as to environment problems [50, 51]. Hydrogen is a non-polluting clean energy carrier that has been considered as a potentially very good energy source in the days to come [52–54]. Li et al. [55]. synthesized CMP photocatalysts in 2020 by embedding diketopyrrolopyrrole (DPP) in triphenylamine (TPA), bipyridine (bdy), as well as biphenyl (bph) building blocks to prepare DPP-bdy-TPA as well as DPP-bph-TPA architectures. DPP has superior light-harvesting capacity due to its planar structure as well as high electron deficiency, giving rise to low bandgap as well as strong π—π stacking. The findings showed that DPP-bdy-TPA exhibited strong photoresponse across a broad spectrum, with apparent quantum yields (AQYs) of 9.60% at 420 nm, 7.32% at

27662098, 2026, 2, Downloaded from https://onlinelibrary.wiley.com/doi/10.1002/EXP.20240487 by CochraneChina, Wiley Online Library on [08/06/2026]. See the Terms and Conditions (https://onlinelibrary.wiley.com/terms-and-conditions) on Wiley Online Library for rules of use; OA articles are governed by the applicable Creative Commons License

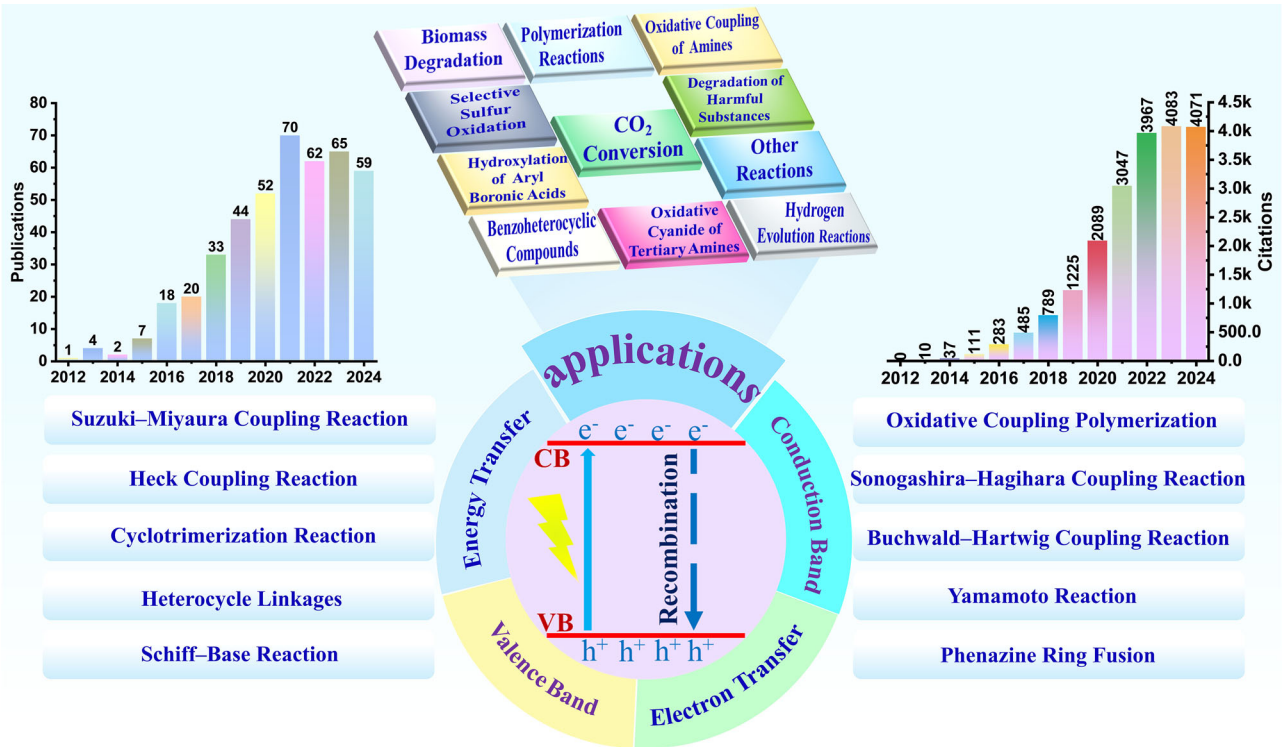


FIGURE 1 | The catalytic mechanism, preparation method, application, annual publication quantity and citation rate of CMPs-based photocatalyst (annual publications and citations on CMP photocatalysts (assessed 21st Nov 2024)).

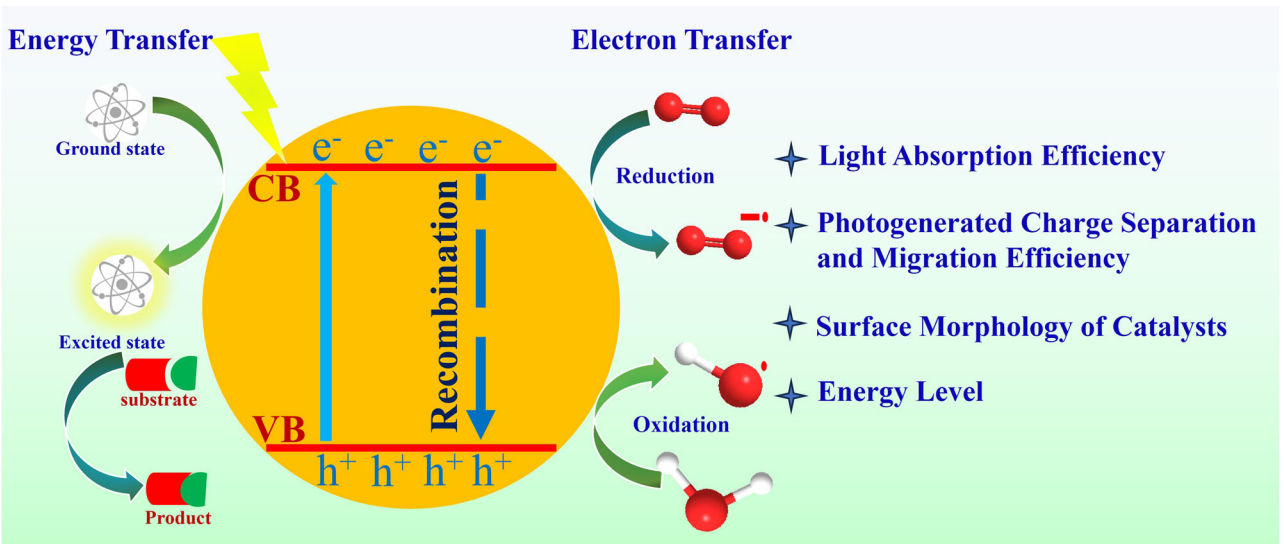


FIGURE 2 | Schematic diagram of photocatalytic process and influencing factors of photocatalytic performance.

500 nm, and 0.31% at 600 nm. Under full-spectrum xenon lamp irradiation and visible light above 440 nm, the hydrogen evolution rates (HERs) reached 6918 μmol g^{-1} h^{-1} for DPP-bdy-TPA and 2780 μmol g^{-1} h^{-1} for DPP-bph-TPA. By comparison, it was found that the hydrophilic bipyridine unit showed better photocatalytic performance. In 2023, Meng et al. [56]. prepared pyridyl-CMPs (*p*-PCMP, *m*-PCMP, *m*-NPCMP) by polycondensation between aldehydes and aryl ketone monomers. Introduction of pyridyl nitrogen atoms enhances molecular-level wettability in CMPs. Because of its small bandgap as well as developed hierarchical porous structure, *m*-PCMP demonstrated outstanding photocatalytic performance in the whole ultraviolet-visible spectroscopy (UV–Vis) region with production rates as 29.86 and 9.56 μmol h^{-1}, respectively. Aside from improved wettability, pyridyl nitrogen enhances swift charge carrier mobility through enhanced transport throughout the π-conjugated skeleton. Additionally, it facilitates tuning of photocatalytic performance through bandgap location as well as width modification.

Carbazole has good chemical and environmental stability as it is entirely aromatic [57]. Its incorporation with a bridging biphenyl unit serves to decrease the bandgap in the formed polymer,

27662098, 2026, 2, Downloaded from https://onlinelibrary.wiley.com/doi/10.1002/EXP.20240487 by CochraneChina, Wiley Online Library on [08/06/2026]. See the Terms and Conditions (https://onlinelibrary.wiley.com/terms-and-conditions) on Wiley Online Library for rules of use; OA articles are governed by the applicable Creative Commons License

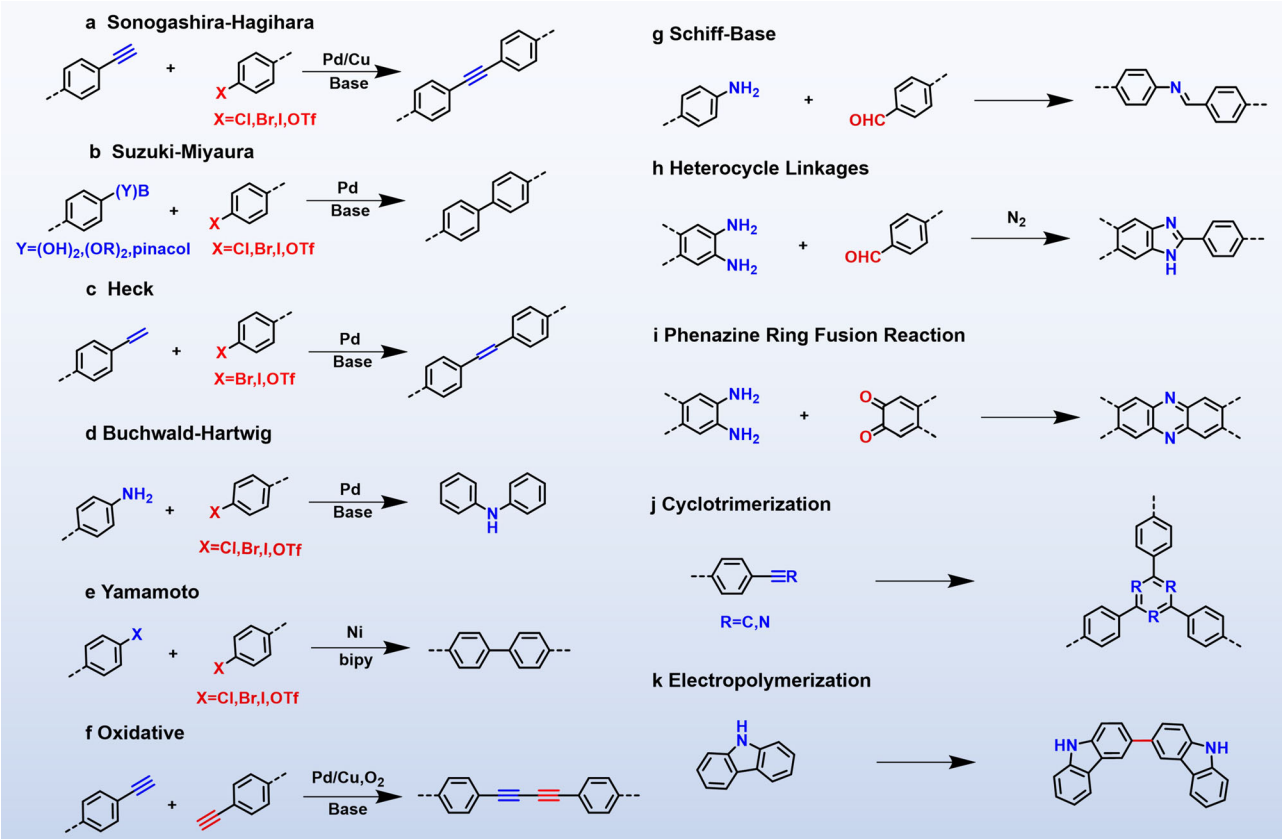


FIGURE 3 | Classical synthesis route of CMPs.

distinguishing polycarbazole from normal polyphenyl systems [58]. Ahmed et al. [59]. in 2021 synthesized two new carbazole-thiophene-based CMPs (e.g., Cz-3Th and Cz-4Th-CMPs) by a Suzuki–Miyaura coupling reaction from characteristic coplanar carbazole precursors (e.g., Cz-3Br and Cz-4Br). This increased efficiency was due to the low extent of branching as well as planar molecular structure that provided increased orbital overlap in the conjugated network, thus enhancing the efficiency of photogenerated charge pair separation.

Following recent studies, dibenzothiphene-S,S-dioxide (BTDO) [60, 61] was discovered to be an exemplary building block for CMP-based photocatalysts owing to the superior electron-withdrawing nature, coplanar structure, as well as hydrophilic character of the sulfone group [62, 63]. Zhang et al. [64]. applied a statistical copolymerization method in 2021 to fine-tune pyrene and BTDO monomers ratios in order to expand the catalytic efficiency of copolymers. An increase in the fraction of BTDO altered polymer parameters, among them the morphology, superficial area, pore size, hydrophilicity and photocatalytic efficiency. When the monomer ratio was tuned to 25:75, the material PyBS-3 displayed strong broad-spectrum light absorption and improved hydrophilicity, yielding a HER of 1.05 mmol h^{-1} under UV–Vis irradiation (λ > 300 nm) with ascorbic acid as the sacrificial donor. In 2022, Jiang et al. [65]. developed two CMP photocatalysts featuring a donor–π–acceptor (D–π–A) structure. These were synthesized using dibenzo[*g,p*]chrysene or pyrene as donor units, thiophene as the π-bridge, and dibenzo[*b,d*]thiphene-S,S-dioxide as the acceptor. Among them, Py-TP-BTDO exhibited effective charge separation and reached an HER of 115.03 mmol h^{-1} g^{-1} under visible light (λ > 420 nm). Outdoor tests further confirmed its activity, with the Py-TP-BTDO membrane (120 cm^2 active area) rapidly producing hydrogen bubbles under natural sunlight. In 2023, Jiang et al. [61]. synthesized a set of CMPs with D–π–A–A structures and varied BTDO contents via ternary statistical copolymerization. Among them, PyT-BTDO-2 exhibited the most effective performance, achieving an HER of H_2 of 230.06 mmol h^{-1} g^{-1} (Figure 4A). This study highlights that designing CMPs with D–π–A–A structure can significantly enhance photocatalytic hydrogen production and underscores the critical role that the proportion of electron-accepting units plays in dictating overall photocatalytic efficiency.

Due to its helical geometry—three benzene units linked to a central nitrogen—TPA is extensively used as an electron donor, recognized for its strong optical performance and excellent conductivity. As a consequence, this has widely applied in luminescent probes as well as in molecular electronics. TPA, in comparison to other aroma-based compounds, provides wide π-conjugation, thus supporting red-shifted absorption as well as emission spectra. The D–π–A structure, which also enjoys superior π-electron delocalization, can additionally enhance the efficiency in the photocatalytic process through lower exciton binding energy as well as easier exciton dissociation. In 2024, Mohamed et al. [35]. designed six CMPs originated from TPA as follows: TPA-TPA (D–D), TPE-TPA (A–D), Py-TPA (A–D), TPA-TB-TPA (D–π–D) TPE-TB-TPA (D–π–A), as well as Py-TB-TPA (D–π–A).From these compounds, Py-TPA as well as Py-TB-TPA provided HERs of 3633 mmol g^{-1} h^{-1} and 16700 mmol g^{-1}

27662098, 2026, 2, Downloaded from https://onlinelibrary.wiley.com/doi/10.1002/EXP.20240487 by CochraneChina, Wiley Online Library on [08/06/2026]. See the Terms and Conditions (https://onlinelibrary.wiley.com/terms-and-conditions) on Wiley Online Library for rules of use; OA articles are governed by the applicable Creative Commons License

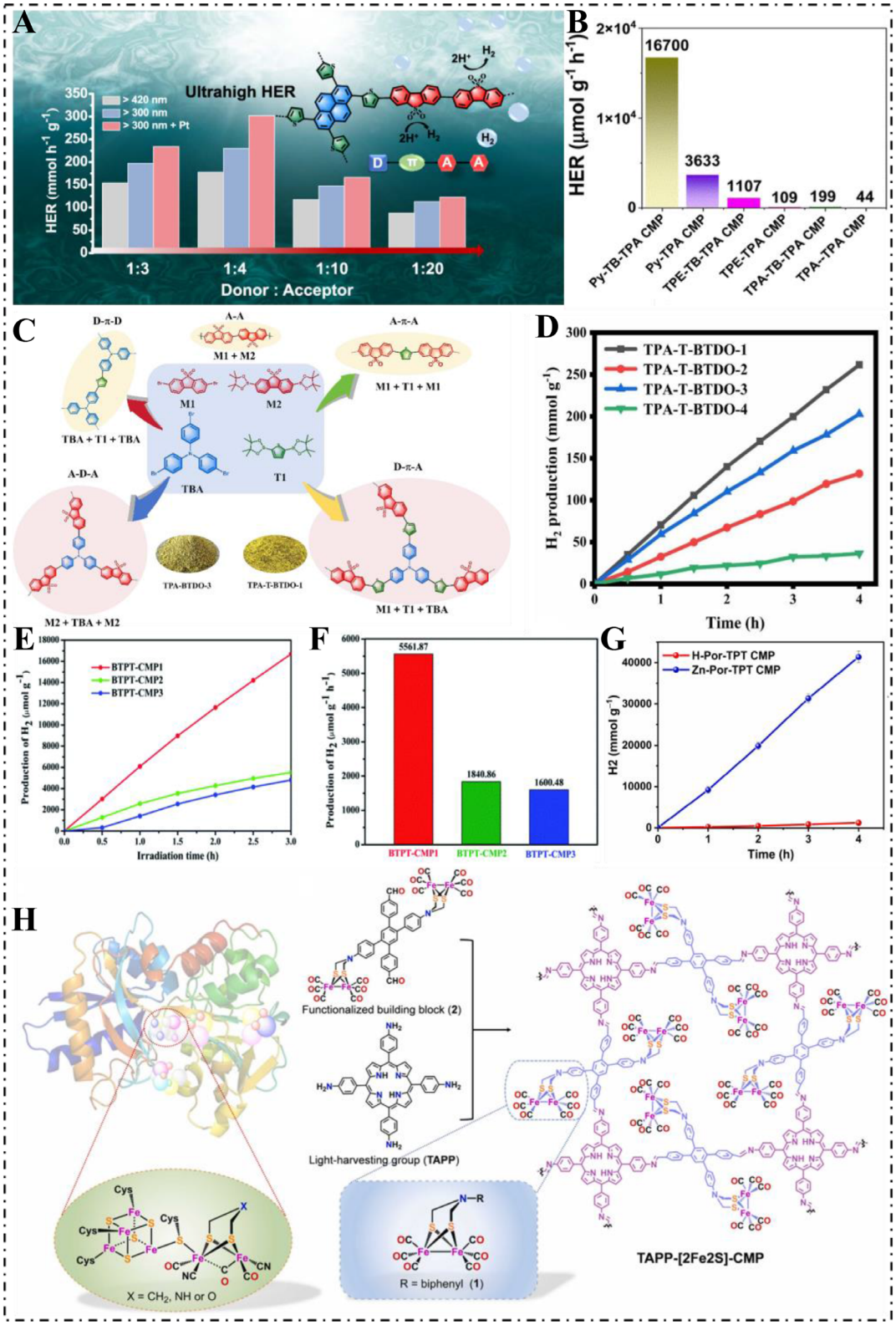


FIGURE 4 | (A) Comparison of photocatalytic properties of D–π–A–A type CMPs. Reproduced with permission [61]. Copyright 2023, American Chemical Society. (B) HER profiles of TPA-TPA, TPE-TPA, Py-TPA, TPA-TB-TPA, TPE-TB-TPA, and Py-TB-TPA CMPs. Reproduced with permission [35]. Copyright 2024, Royal Society of Chemistry. (C) Synthetic routes and possible conceptual structures of TPA-BTDO-3 and TPA-T-BDTO-1 CMP. (D) HER rates of TPA-T-BTDO-1, TPA-T-BTDO-2, TPA-T-BTDO-3 and TPA-T-BTDO-4 under visible light ($\lambda > 420$ nm). Reproduced with permission [66]. Copyright 2024, Elsevier Ltd. (E) HER of the three polymers under visible light. (F) The H_2 production rates of the three polymers. Reproduced under the terms of the Creative Commons CC-BY license [67]. Copyright 2022, The Authors. (G) The photocatalytic long-term stability of Zn-Por-TPT CMP. Reproduced with permission [68]. Copyright 2023, Elsevier Ltd. (H) The constructing the framework of TAPP-[2Fe2S]-CMP and the structure of its functional sites. Reproduced with permission [69]. Copyright 2023, Elsevier Ltd.

27662098, 2026, 2, Downloaded from https://onlinelibrary.wiley.com/doi/10.1002/EXP.20240487 by CochraneChina, Wiley Online Library on [08/06/2026]. See the Terms and Conditions (https://onlinelibrary.wiley.com/terms-and-conditions) on Wiley Online Library for rules of use; OA articles are governed by the applicable Creative Commons License

h^{-1}, respectively (Figure 4B). Theoretical models exposed that through having alkyne linkers in Py-TB-TPA, electron–hole pair recombination can effectively decrease, charge carrier lifetime can prolong as well as transfer as well as separation efficiency can increase. A novel design strategy was presented by Zhang et al. [66]. in 2024, where the propeller-like 3D structure of TPA acted as the donor and BTDO as the acceptor to form the macrocyclic D–A CMP catalyst TPA-BTDO (Figure 4C). Incorporating thiophene units into the framework further enhanced planarity between the donor and acceptor components. This modification led to the development of TPA-T-BTDO-1, which exhibited impressive photocatalytic HER, reaching 65.41 mmol h^{-1} g^{-1} under visible irradiation (Figure 4D). The unique twisted arrangement of TPA minimized the dihedral angle relative to BTDO, resulting in a more coplanar backbone and enhanced dissociation of photogenerated electron–hole pairs. This structural adjustment inhibits charge recombination along the polymer chain and highlights the critical role of the donor geometry in influencing photocatalytic activity.

The presence of nitrogen in the triazine unit enhances hydrophilicity, making triazine an effective electron-accepting component for designing D–A structured CMPs aimed at photocatalytic hydrogen production. In 2022, Dong et al. [67]. developed three triazinyl D–A CMPs based on different thiophene unit crosslink lengths. BTPT-CMP1 demonstrated superior photocatalytic capacities, in the form of blue-shifted light consumption, enhanced photocurrent, as well as increased HER of 5561.87 mmol h^{-1} g^{-1} (Figure 4E,F). Many studies indicated that crosslink length in CMPs is very critical in relation to pushing their photocatalytic effectiveness. Mohamed et al. [70]. in 2024 outlined two new CMPs, whose designs encompassed utilization of thienyltriazine (TTh) moieties. These CMPs were tailored specifically for energy storage, as well as photocatalytic hydrogen production under visible light. Very importantly, PyT-TTh CMP demonstrated rapid charge separation as well as low recombination losses due to which their high production capacity for hydrogen was very significant, specifically 18,533 μmol h^{-1} g^{-1} under hydrolysis conditions. In 2024, Zhang et al. [68]. developed two triazine-porphyrin-based CMPs—H-Por-TPT and Zn-Por-TPT. The introduction of Zinc ions significantly enhanced the photocatalytic activity, leading to a redshift in light absorption and achieving a HER of up to 11450 μmol h^{-1} g^{-1} under visible light (Figure 4G). Yan et al. [69]. reported the synthesis of another CMP, TAPP-[2Fe2S]-CMP, via Schiff base condensation using a [FeFe]-hydrogenase model complex. With a HER of 2120 μmol h^{-1} g^{-1} (Figure 4H), this photocatalyst shows considerable promise for developing sustainable and high-efficiency systems that minimize reliance on nonrenewable resources.

3.2 | CO_2 Conversion

The accelerated pace of industrialization and human activity has resulted in the extensive use of fossil fuels, significantly elevating greenhouse gas emissions—particularly carbon dioxide—which has triggered severe energy and environmental challenges. Taking inspiration from natural photosynthesis, researchers have designed artificial systems that harness solar energy to transform carbon dioxide (CO_2) into valuable products such as methane (CH_4), methanol (CH_3OH), and formic acid (HCOOH) [71], while simultaneously driving water oxidation to release O_2 [72, 73]. These artificial photosynthetic approaches are considered among the most effective strategies for reducing CO_2 emissions. Among photocatalysts for CO_2 conversion, inorganic semiconductor materials such as titanium dioxide (TiO_2) [71, 74] and cadmium sulfide (CdS) [75] have been widely investigated for the realization of the CO_2 photoreduction process. For this technology to reach commercial viability, substantial enhancements are still needed in the photocatalyst's light absorption capabilities, product selectivity, and overall solar energy conversion efficiency.

To maximize solar spectrum utilization, Soumitra et al. [76]. in 2021 designed a metal-free photocatalyst that operates under visible light to reduce CO_2 into methane. they successfully synthesized a redox-active CMP named TPA-PQ (Figure 5A). To elucidate its photocatalytic mechanism, density functional theory (DFT) calculations were performed (Figure 5B). The material's porosity was confirmed using Brunauer–Emmett–Teller (BET) analysis, which revealed a surface area of 492 m^2 g^{-1} (Figure 5C). Additionally, TPA-PQ achieved a CO_2 uptake of 30 cm^3 g^{-1} (Figure 5D), indicating its strong potential for use in photocatalytic CO_2 fixation and transformation. The excellent CO_2 adsorption capacity makes TPA-PQ and TEB-PQ ideal candidates as non-homogeneous media suitable for CO_2 photoreduction. TPA-PQ demonstrated exemplary visible-light-driven CO_2 reduction performance, producing 32.2 mmol g^{-1} of methane in 16 h (Figure 5E), with maximum turnover number (TON) as high as 40.5 in the same time period. The rate of production for methane was up to as much as 2.15 mmol g^{-1} h^{-1}, with selectivity over 97% (Figure 5F). Low levels of hydrogen were also found to accumulate in the process of the reaction. This article outlines a promising avenue towards designing extremely efficient heterogeneous photocatalysts, offering practical solutions to environmental challenges as part of the general solution to the world energy crisis.

To broaden the scope of applications and light absorption capabilities of CMP materials, in 2022, Wu et al. [77]. constructed three CMPs with intramolecular D–A structures (P1, P2, P3) by combining electron-donating pyrene and electron-accepting fluorenone derivatives in a polymer network. The three polymers exhibited significant light absorption over a broad spectral range of 350 to 1000 nm (Figure 5G) and had a narrow energy gap of 1.61 to 1.74 eV (Figure 5H). By employing triethanolamine (TEA) and 1-benzyl-1,4-dihydronicotinamide (BNAH) as sacrificial agents, the P3 CMP demonstrated the highest photocatalytic activity under visible light, achieving carbon monoxide and methane production rates of 932.9 and 943.4 μmol h^{-1} g^{-1}, respectively (Figure 5I). Under red-light irradiation, P3 continued to perform effectively, yielding CH_4 and CO at rates of 293.7 and 282.6 μmol h^{-1} g^{-1} (Figure 5J), with nearly complete reaction selectivity. The enhanced performance of P3 over P1 and P2 is linked to its greater CO_2 uptake capacity and more effective photoinduced charge transfer. This study provides an encouraging avenue to the development of CMPs responsive to wide spectra for sunlight-efficient CO_2 conversion.

Besides the light-harvesting ability of the photocatalytic material, in CO_2 photoreduction, structure design on CMP also affects efficiency. Zhao et al. [78]. in 2022 designed a new series of ion-CMPs from imidazolium salts (ImI-CMPs), which enhanced CO_2 reduction under visible light dramatically by boosting

27662098, 2026, 2, Downloaded from https://onlinelibrary.wiley.com/doi/10.1002/EXP.20240487 by CochraneChina, Wiley Online Library on [08/06/2026]. See the Terms and Conditions (https://onlinelibrary.wiley.com/terms-and-conditions) on Wiley Online Library for rules of use; OA articles are governed by the applicable Creative Commons License

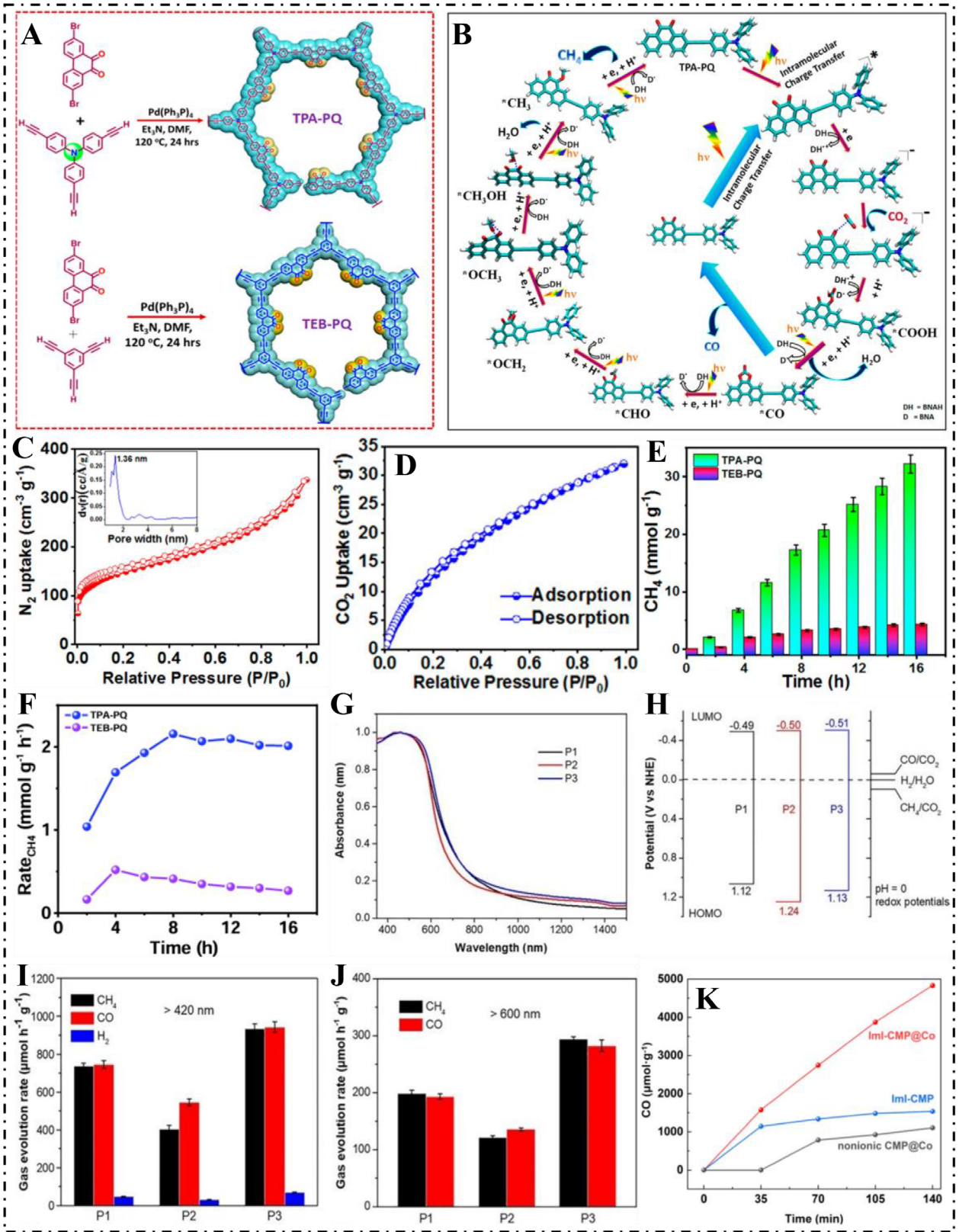


FIGURE 5 | (A) Illustration of synthesis pathways of TPA-PQ and TEB-PQ via C—C coupling reactions. (B) Proposed catalytic mechanism depicting key intermediates involved throughout the photocatalytic cycle. (C) Adsorption isotherm of TPA-PQ at 77 K for N_2 (in the inset; pore size distribution). (D) CO_2 adsorption isotherm of TPA-PQ at 298 K. (E) Time-dependent formation of CO_2 reduction products in MeCN-H_2O (F) Comparison of CH_4 production rates between TPA-PQ and TEB-PQ under similar reaction conditions. Reproduced with permission [76]. Copyright 2021, American Chemical Society. (G) Normalized UV–vis–NIR absorption spectra. (H) Band alignment of the three polymers at pH = 0. Photocatalytic activity of the CMPs for CO_2 reduction upon (I) visible light and (J) red light irradiation. Reproduced with permission [77]. Copyright 2022, Wiley-VCH. (K) Photocatalytic evolution of CO by ImI-CMP@Co, ImI-CMP and nonionic CMP@Co. Reproduced with permission [78]. Copyright 2021, Elsevier Ltd.

27662098, 2026, 2, Downloaded from https://onlinelibrary.wiley.com/doi/10.1002/EXP.20240487 by CochraneChina, Wiley Online Library on [08/06/2026]. See the Terms and Conditions (https://onlinelibrary.wiley.com/terms-and-conditions) on Wiley Online Library for rules of use; OA articles are governed by the applicable Creative Commons License

intramolecular charge transfer (ICT). Complementing the structure of ImI-CMPs with Co(II) ions enhanced performance even more to reach carbon monoxide (CO) production rates up to 2953 μmol g^{-1} h^{-1} as well as turnover frequencies up to 30.8 h^{-1} (Figure 5K). DFT calculations confirmed that easy CO_2 activation owing to imidazole moieties in conjunction with rapid photoinduced electron transfer (PET) facilitated through π-conjugation as well as inner electric field in polymer controlled performance greatly. This research opens powerful strategy avenues towards sophisticated organic photocatalytic designs through cationic imidazole substructure integration into conjugated systems as well as points to the cooperative role that metal ion integration can contribute towards enhancing CO_2 photoreduction efficiency. Rahimi et al. [79]. synthesized TEB-BPY CMPs by C—C coupling polymerization and prepared Re@TEB-BPY metal hybrid polymers for photocatalytic CO_2 reduction utilizing the coordination ability of bipyridine with [$Re(CO)_5Cl$] (Figure 6A). Employing TEA as a sacrificial donor resulted in CO formation at 91.7 μmol g^{-1} h^{-1} with 68% selectivity. Substituting BNAH as the sacrificial agent and maintaining TEA as the base redirected the reaction toward methane, achieving 2.05 mmol g^{-1} h^{-1} with approximately 96% selectivity and a quantum efficiency of 0.22% (Figure 6B). Mechanistic insights were obtained through in situ diffuse reflectance Fourier transform infrared spectroscopy (DRIFTS) analysis and DFT modeling. From these studies, as well as controlled experiments, it is understood that TEA is extremely crucial in back electron transfer suppression when BNAH is added, consequently enhancing the overall efficiency in the photocatalytic process. This work improved the CO_2 photoreduction yield by introducing metal ions, which provides the basis and theoretical foundation for the synthesis of metal-hybridized CMPs.

The photocatalytic reduction of CO_2 to CH_4 not only needs to be considered with high conversion efficiency but also should ensure high selectivity to reduce the generation of by-products. In 2023, Meng et al. [80]. achieved a CO_2 photoreduction selectivity of 71.2% through rational adjustment of the donor as well as acceptor structure in the CMP structure. To establish an effective donor–π–acceptor (D–π–A) framework, the researchers strategically synthesized two redox-active truxene based CMPs—Tx-TzTz-CMP-1 and Tx-TzTz-CMP-2—incorporating thiazolyl [5,4-*d*] thiazole linkers (Figure 6C). Of the two, Tx-TzTz-CMP-2—with its extended π-conjugated—delivered a methane yield of 300.6 μmol g^{-1} h^{-1}. BET analyses also confirmed their large surface area of 654 and 676 m^2 g^{-1}, respectively. Experimental measurement as well as theory calculation confirmed that conversion from D–A architecture to D–π–A structure can effectively drive ICT as well as carrier separation. Apart from Apart from that, the nitrogen atom in the thiazole group acts as electron reservoir as well as catalytic site to facilitate CO_2 activation as well as reduced hydrogenation to produce methane. This study offers feasible guidance to rationally engineer the photo-catalysts with high CO_2 to CH_4 conversion selectivity.

3.3 | Biomass Valorization

Biomass serve as a renewable source of organic material that can be converted intonumerous valuable chemical products. Although precious metal catalysts are frequently utilized in such catalytic processes, their widespread application—combined with the need for elevated temperatures and pressures—leads to high energy demands and increased operational costs. [83–85] Consequently, the development of intelligently designed photocatalysts, utilizing sunlight as the catalytic energy source, offers a promising approach to replacing the harsh reaction conditions and costly catalytic redox processes traditionally associated with biomass valorization [86].

In 2021, Ma et al. [81]. synthesized a group of CMPs by linking 2,4,6-(tri-2-thiophenyl)-1,3,5-triazine (TTT) with three different linker units—benzothiadiazole (BTD), benzene (Ben), and dimethoxybenzene (DMOB)—producing the materials pTTT-BTD, pTTT-Ben, and pTTT-DMOB, respectively (Figure 6D). These linkers significantly influenced the morphology, optical behavior, electrical conductivity, and photocatalytic activity of the resulting CMPs. These CMPs were utilized in biomass conversion processes, effectively catalyzing the hydrogenation of maleic acid into succinic acid with a production rate of 4.66 mmol g^{-1} h^{-1} (Figure 6E), and facilitating the light-driven oxidation of 5-hydroxymethylfurfural (HMF) to 2,5-diformylfuran (DFF) at a rate of 0.53 mmol g^{-1} h^{-1} (Figure 6F). These results highlight the promise of carefully engineered CMPs as sunlightresponsive photocatalysts for the sustainable transformation of biomass-based feedstocks.

In 2023, Huang et al. [82]. designed a D–A CMP photocatalyst that was optimized structurally on the atomic level to increase charge separation in addition to overall efficiency as a photocatalyst. The compound integrated thiophene as the electron donor moiety while the acceptors were aryl *N*-heterocycles. Through tuning in nitrogen content in acceptors, the polymer was in a position to fine-tune the electron affinity to vary the band structure in addition to the polymer's exciton binding energy. Interestingly, through embedding s-triazine into the polymer chain, extensive D–A interaction was formed, significantly enhancing electron delocalization in addition to reducing exciton binding energy to provide superior photocatalytic performance (Figure 6G). Therefore, the resulting CMP-Tz exhibited significantly improved charge-separation efficiency. To study the oxidation pathway of HMF, in situ electron paramagnetic resonance (EPR) spectroscopy was employed with 5,5-dimethyl-1-pyrroline-*N*-oxide (DMPO) as a spin trap to capture and identify reactive radicals. CMPs form and separate photoexcited holes as well as electrons on their surface under light. Electrons are transferred to a platinum cocatalyst to convert protons to gaseous hydrogen in aqueous solution. The holes, however, oxidize HMF by abstracting one electron and one proton from the α–C–H site to yield detectable HMF radicals by EPR. When tested with ascorbic acid as a sacrificial agent, CMP-Tz exhibited a maximum HER of 3207 μmol g^{-1} h^{-1} (Figure 6H). Furthermore, CMP-Tz enabled dual hydrogen evolution as well as extremely selective stoichiometric HMF oxidation to DFF (Figure 6I). The report presents pioneering protocols for systematic polymer-supported photocatalytic designs that can accomplish their dual roles in solar fuel production as well as biomass-derived chemical valorization.

3.4 | Polymerization Reactions

Photochemistry is gaining significance as a green approach of polymer synthesis with accurate structural control,

27662098, 2026, 2, Downloaded from https://onlinelibrary.wiley.com/doi/10.1002/EXP.20240487 by CochraneChina, Wiley Online Library on [08/06/2026]. See the Terms and Conditions (https://onlinelibrary.wiley.com/terms-and-conditions) on Wiley Online Library for rules of use; OA articles are governed by the applicable Creative Commons License

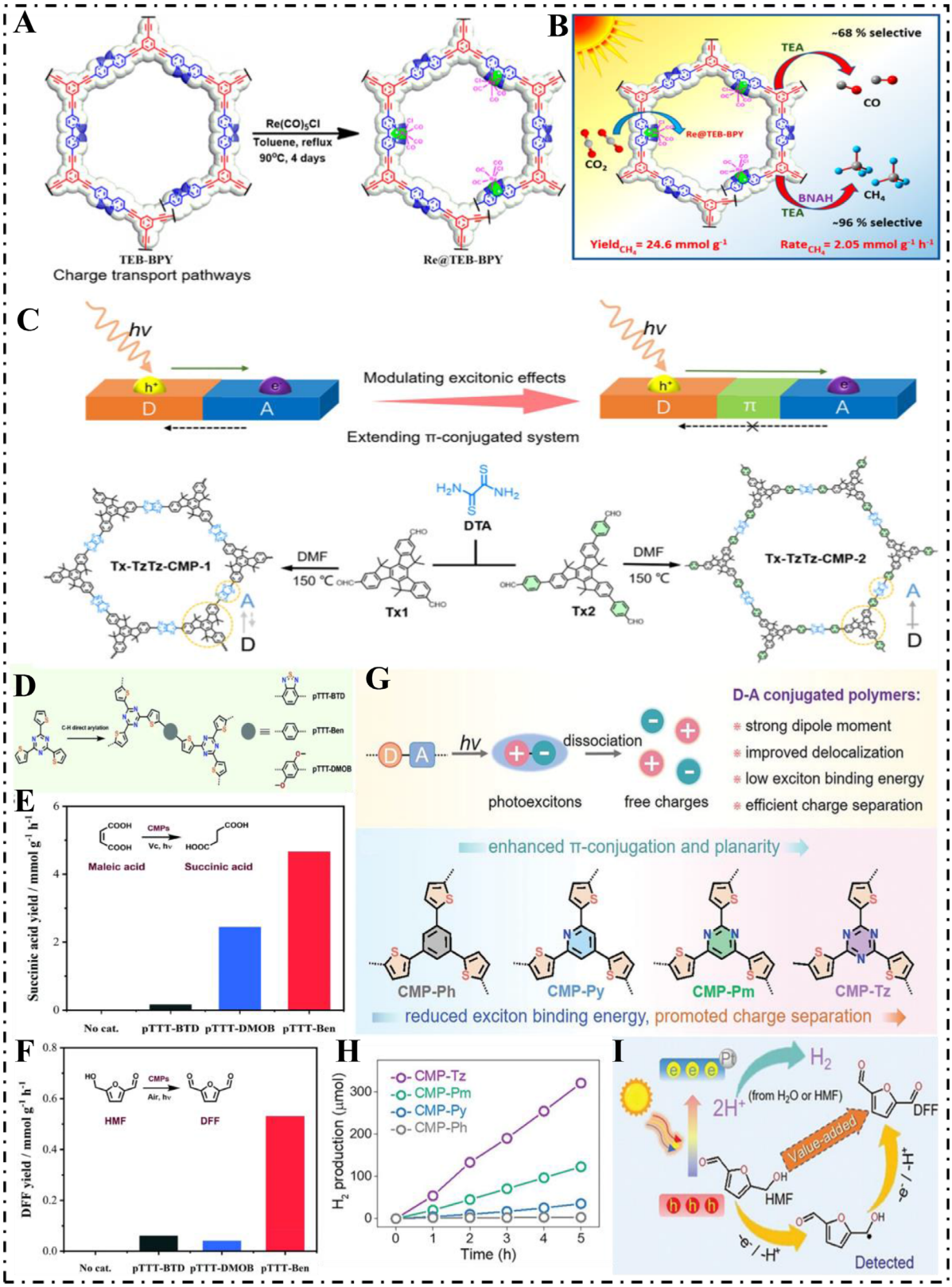


FIGURE 6 | (A) Synthetic scheme for the preparation of Re@TEB-BPY. (B) General overview of photocatalytic CO_2 reduction based on Re(I)-Integrated CMPs. Reproduced with permission [79]. Copyright 2023, American Chemical Society. (C) Schematic diagrams of photoexcited charge transport paths of Tx-TzTz-CMP-1 and Tx-TzTz-CMP-2 materials based on D–A and D–π–A systems and their synthetic routes. Reproduced with permission [80]. Copyright 2023, American Chemical Society. (D) Synthetic routes of CMPs. Photocatalytic production rates of succinic acid (E) and DFF (F) with different catalysts. Reproduced with permission [81]. Copyright 2021, Royal Society of Chemistry. (G) Schematic diagram of the design of CMPs. (H) Photocatalytic H_2 production of CMPs in the presence of 0.1 M ascorbic acid. (I) Proposed reaction mechanism for the oxidative conversion of HMF to DFF. Reproduced with permission [82]. Copyright 2023, Wiley-VCH.

27662098, 2026, 2, Downloaded from https://onlinelibrary.wiley.com/doi/10.1002/EXP.20240487 by CochraneChina, Wiley Online Library on [08/06/2026]. See the Terms and Conditions (https://onlinelibrary.wiley.com/terms-and-conditions) on Wiley Online Library for rules of use; OA articles are governed by the applicable Creative Commons License

introducing spatiotemporal control of polymer chain propagation and development of complex polymeric materials [43]. Various of these photocatalytic processes have been developed to activate new chemical transformations and allow controlled syntheses of polymers of well-defined structures using light energy. Through photoinduced polymerization, the photoexcited states of the photocatalysts dictate electron or energy transfer processes activating polymer chains directly and allowing controlled steps of initiation and termination [87]. Techniques like PET-RAFT, atom transfer radical polymerization (ATRP), and other photoinduced radical polymerizations rely on photocatalysts to modulate both the initiation and termination stages of polymer chain formation [88].

For effective use of long-wavelength visible light sources in ATRP, it is essential to devise proper photocatalytic systems that can connect PET processes along with ATRP components and then activate controlled/living polymerization [44]. Matyjaszewski et al. [89]. prepared a dual catalyst system of phenothiazine-based CMPs (PTZ-CMPs) utilized as a heterogeneous photocatalyst and a copper catalyst utilized to manage ATRP under green and red light in 2021 (Figure 7A). Using dimethoxybenzene (DMOB) utilized as a crosslinking agent, the PTZ subunits were embedded within a photoresponsive network using a Friedel–Crafts reaction and prepared PTZ-CMPs with visible-light functionality based on the extended aromatic skeleton that encircles the PTZ cores (Figure 7B). Under green or red light irradiation, these of CMP-based photocatalysts activate Cu-catalyzing ATRP and result in proper polymerization of methacrylate and acrylate monomers at high conversion rates and molecular weight control.

Light-induced continuous flow reactors have emerged as a reliable and sustainable method for the production and processing of small and large molecules to facilitate efficient and homogeneous irradiation pathways. Despite significant advances, available homogeneous photocatalysts are still constrained by weaknesses that prevent widespread adoption of this technology [93]. To overcome these weaknesses, Cai et al. [90]. prepared hollow nanotube CMPs (*h*PorBDP NTs) of silica nanorod sacrifice templates using Sonogashira–Hagihara cross-coupling polycondensation in 2023. Prepared nanotubes were of hollow cores and high porosity and facilitated charge separation and abundant accessible catalytic sites for photocatalytic processes (Figure 7C,D). These CMP nanotubes were efficient catalysts and were used successfully for PET-RAFT polymerization of acrylates and acrylamide and were found to yield excellent molecular weight distribution control. In 2024, Cai et al. [91]. challenged the low dispersibility of aqueous-phase photopolymerizations under continuous flow by preparing hairy hollow CMPs nanocomposites (S-*h*EBDT-P HCMPs) via a template–directed method (Figure 7E). They revealed these HCMPs exhibited remarkable water dispersibility and strong resistance toward oxygen and were observed to serve as effective heterogeneous catalysts for accelerating PET-RAFT reactions under batch and continuous-flow processes. Optimum reaction conditions made it possible to repetitively use the catalyst S-hEBDT-P and scale up poly(4-acryloylmorpholine) (PAMPs) productions at high output and low molecular weight distributions using flow reactors (Figure 7F). This work forms the foundation of fine-tuning PET-RAFT polymerization using flow processes toward developing intelligent and tunable catalytic platforms of use for high-value polymer synthesis on a scale-up basis.

3.5 | Degradation of Harmful Substances

With the rapid and vigorous development of modernization, a large number of harmful substances are being produced by human activities [36, 94–96]. These hazardous chemicals are real threats to the health of humankind and can cause lasting and irreparable harm to the environment. Therefore, it is essential that those treatment processes which are not only highly effective but at the same time cost- and energy-saving and eco-friendly are developed and designed intricately. To this end, photochemistry has been considered as an ideal route for the light-driven degradation of harmful substances.

In 2022, Chen et al. [97]. designed a visible-light-responsive CMP photocatalyst called pTTT-Ben, capable of extracting U(VI) from highly acidic environments. The study examined the effects of various hole scavengers on the photocatalytic reduction process and determined that ascorbic acid was the most efficient in enhancing U(VI) removal. Its strong reduction potential and strong interaction with the basic nitrogen atoms in pTTT-Ben likely contributed to the highest U(VI) removal efficiency observed. The photocatalyst exhibited visible light absorption in the 500–600 nm range and had an optical bandgap of 2.50 eV, enabling the reduction of U(VI) under natural sunlight. Under environmental conditions averaging 27.1°C with solar intensity at 1181.9 W m^{-2}, pTTT-Ben achieved an 82% U(VI) removal rate within 8 h. Furthermore, selectivity tests involving 11 competing metal ions demonstrated that pTTT-Ben maintained good selectivity, achieving 60% U(VI) removal under light irradiation. The exceptional stability and conjugated structure of pTTT-Ben enabled it to sustain efficient photocatalytic reduction under highly acidic environments (pH = 1), with a removal capacity of 4710 mg g^{-1}. This study demonstrated the removal of hazardous substances in a strongly acidic environment and established the fundamentals for the design of photocatalysts for CMPs adapted to harsh environments.

In 2022, Yu et al. [92]. designed a CMP photocatalyst (ECUT-AQ) incorporating anthraquinone (AQ) as the acceptor and perylene as the donor, aiming to create a D–A system that enhance solar spectrum utilization and promotes efficient electron–hole separation. AQ with strong electron-deficient character and redox ability is the essential functional group of ECUT-AQ and works significantly within its photocatalytic performance (Figure 7G). Nitrogen adsorption–desorption studies at 77 K confirmed that the material had a high BET surface area of 1157.6 m^2 g^{-1} (Figure 8A). Its bandgap, as determined by Tauc analysis, was 1.98 eV, which is lower than the 2.50 eV observed in the CMP previously described by Chen et al. [97]. Additionally, it showed broad absorption from 400 to 800 nm, with a strong peak at 537 nm (Figure 8B,C). ECUT-AQ achieved a uranium (U(VI)) removal of 73% at photoirradiation at pH = 4 and was still featured with 65% efficiency when it was challenged under highly acidic media (pH = 1) under exposure of 60 min. Compared with this, only 15.3% of uranium was removed when it was challenged under darkness and 49.7% of the removal was contributed by the photocatalytic reduction. It is suggested that reduction of AQ led to oxoanthraquinone (OAO) formed under acidic media and then gets reoxidized back to AQ when it came into contact with cavities formed by the material. This redox cycle enables hole consumption and prevents electron–hole recombination and is

27662098, 2026, 2, Downloaded from https://onlinelibrary.wiley.com/doi/10.1002/EXP.20240487 by CochraneChina, Wiley Online Library on [08/06/2026]. See the Terms and Conditions (https://onlinelibrary.wiley.com/terms-and-conditions) on Wiley Online Library for rules of use; OA articles are governed by the applicable Creative Commons License

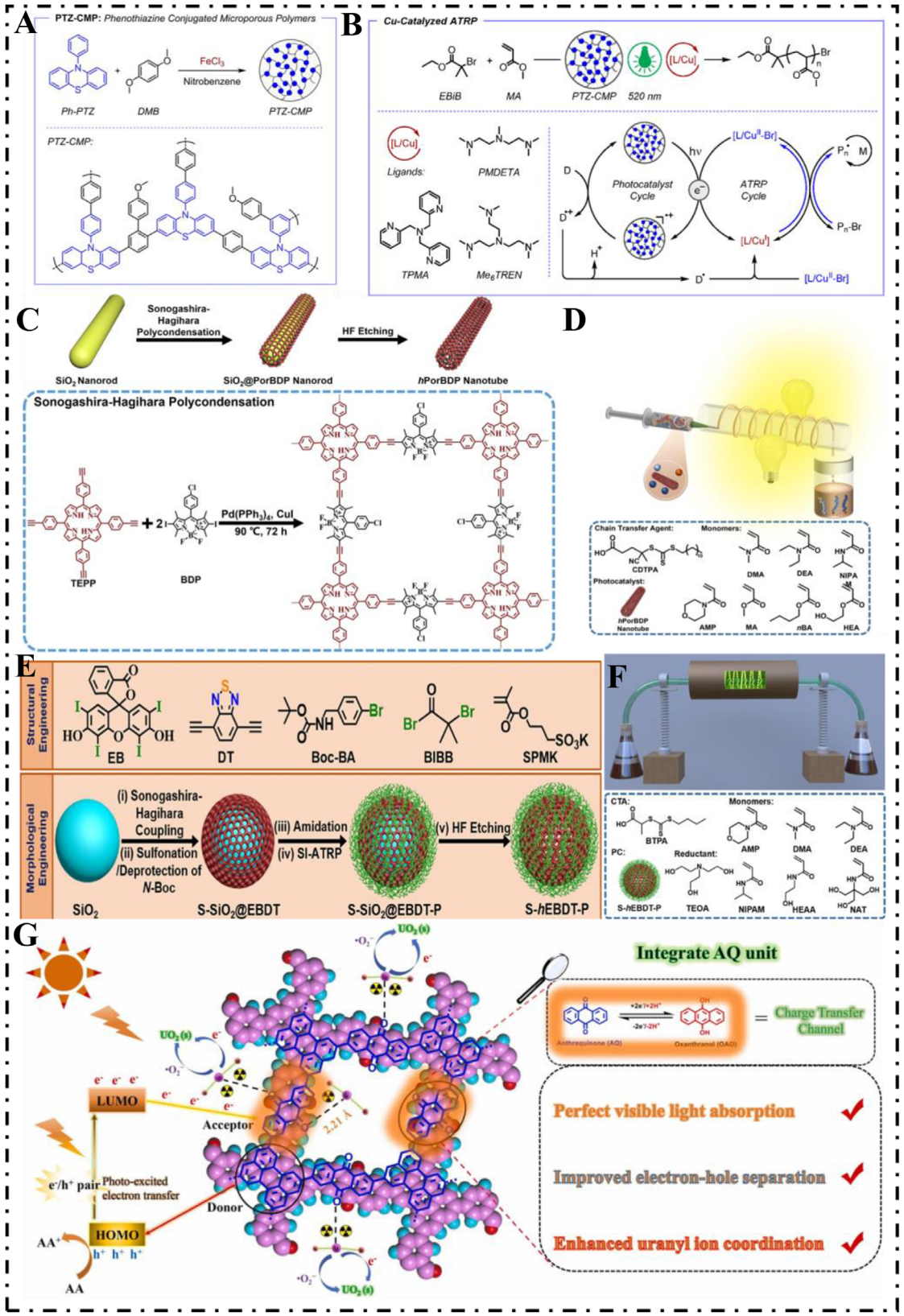


FIGURE 7 | (A) Synthesis of PTZ-CMP. (B) Mechanistic process of photo-induced copper catalysis of ATRP using PTZ-CMP as a heterophase photocatalyst. Reproduced with permission [89]. Copyright 2021, American Chemical Society. (C) Synthetic routes for *h*PorBDP nanotube. (D) Schematic representation of PET-RAFT polymerization catalyzed by *h*PorBDP. Reproduced with permission [90]. Copyright 2023, Elsevier Ltd. (E) Synthetic pathway of S-*h*EBDT-P HCMPs. (F) Schematic representation of PET-RAFT polymerization catalyzed by S-*h*EBDT-P. Reproduced with permission [91]. Copyright 2024, American Chemical Society. (G) The proposed photocatalytic U(VI) reduction mechanism of the **ECUT-AQ**. Reproduced with permission [92]. Copyright 2022, Elsevier Ltd.

27662098, 2026, 2, Downloaded from https://onlinelibrary.wiley.com/doi/10.1002/EXP.20240487 by CochraneChina, Wiley Online Library on [08/06/2026]. See the Terms and Conditions (https://onlinelibrary.wiley.com/terms-and-conditions) on Wiley Online Library for rules of use; OA articles are governed by the applicable Creative Commons License

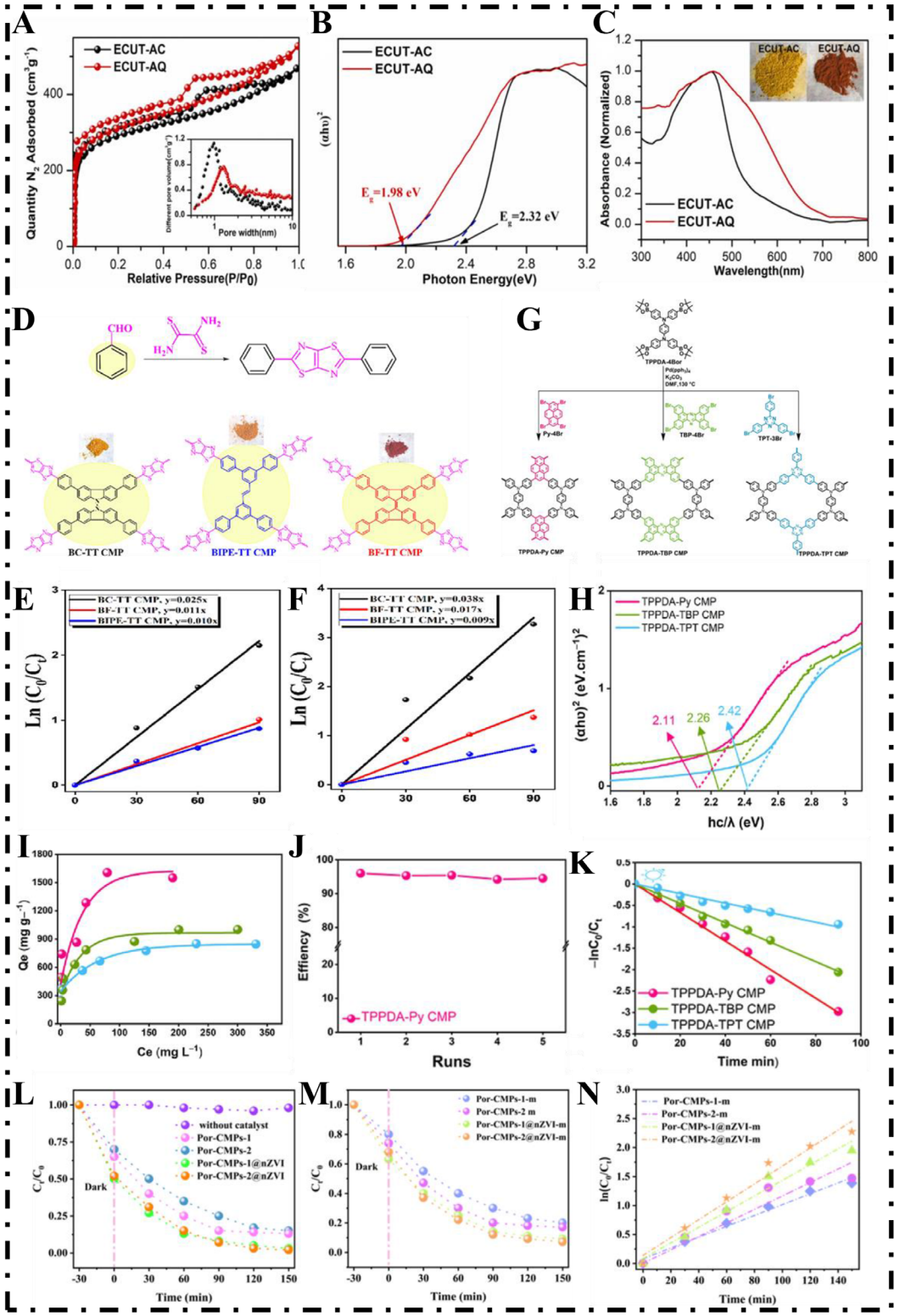


FIGURE 8 | (A) Nitrogen adsorption/desorption curves at 77 K, and the corresponding pore size distribution curves of ECUT-AC and ECUT-AQ via NLDFT calculation (inset). (B) The bandgaps of ECUT-AC and ECUT-AQ calculated by Tauc-plot. (C) UV–Vis DRS spectra of ECUT-AC and ECUT-AQ, inset: apparent color. Reproduced with permission [92]. Copyright 2022, Elsevier Ltd. (D) Synthetic scheme for thiazolyl-linked CMPs. Pseudo-first-order kinetic curves of photocatalytic degradation of RhB (E) and MB (F) in aqueous solutions. Reproduced with permission [98]. Copyright 2023, Elsevier Ltd. (G) Synthetic routes and structures of TPPDA-Py, TPPDA-TBP and TPPDA-TPT CMP. (H) Tauc-plots calculated from UV–Vis spectra of TPPDA-Py, TPPDA-TBP, and TPPDA-TPT CMPs. (I) Langmuir isothermal models of RhB adsorption onto CMPs. (J) Reuse validity of TPPDA-Py CMP for the photodegradation of RhB aqueous solution. (K) Pseudo-first-order kinetics of CMPs for the photodegradation of RhB aqueous solution. Reproduced with permission [99]. Copyright 2023, Elsevier Ltd. (L) and (M) Photocatalytic effect of four different photocatalysts on MB degradation at different times. (N) pseudo-first-order kinetic curves of photocatalytic degradation on MB. Reproduced with permission [100]. Copyright 2024, American Chemical Society.

27662098, 2026, 2, Downloaded from https://onlinelibrary.wiley.com/doi/10.1002/EXP.20240487 by CochraneChina, Wiley Online Library on [08/06/2026]. See the Terms and Conditions (https://onlinelibrary.wiley.com/terms-and-conditions) on Wiley Online Library for rules of use; OA articles are governed by the applicable Creative Commons License

assisted using a sacrificial agent. This work proposed a new D–A based CMP with exceptional uranium reduction ability when it is challenged under extreme acid media and it is a useful guide of designing effective metal-free photocatalysts that can direct wastewater treatment of radioactive wastewater.

Organic dyes dissolved in water are notoriously difficult to eliminate and can severely pollute aquatic environments [101]. In 2023, Kuo et al. [98]. proposed a synthetic strategy for crafting thiazole-linked CMPs incorporating bicarbazole, difluorene, and biphenylene units—named bicarbazole–thiazole-thiazole (BC-TT), bifluorene-thiazole-thiazole (BF-TT), and biphenylene–thiazole-thiazole (BIPE-TT) CMPs, respectively (Figure 8D). These CMPs demonstrated high porosity, with a BET surface area of 522 $m^2\ g^{-1}$, and excellent thermal stability, confirmed by T_{d10} = 460°C and a carbon yield of 67%. Among the synthesized materials, BC-TT CMP exhibited outstanding adsorption capabilities for removing organic dyes such as Rhodamine B (RhB) and methylene blue (MB), with uptake capacities of 228.83 and 232.02 mg g^{-1}, respectively, and corresponding catalytic rates constants of 2.5×10^{-2} and 3.5×10^{-2} min^{-1} (Figure 8E,F). EL-Mahdy et al. [99]. developed an innovative set of D–A type CMPs based on tetraphenyl-*p*-phenylenediamine (TPPDA-CMP) (Figure 8G). These materials demonstrated excellent properties, including high thermal stability (T_{d10} = 546°C), a carbon yield of 74.5%, a surface area reaching up to 1430 $m^2\ g^{-1}$, and a narrow bandgap of 2.11 eV (Figure 8H). Notably, TPPDA- Py-CMP showed an exceptional RhB adsorption capacity of 1587 mg g^{-1} at room temperature (Figure 8I) and achieved nearly complete photocatalytic degradation of RhB with 99% efficiency (Figure 8J) accompanied by a rate constant of 3.3×10^{-2} min^{-1} (Figure 8K). Overall, the results establish D–A type CMPs as strong candidates for photocatalytic removal of organic dye contaminants from wastewater.

The use of superoxide radicals is a reliable method for the photodegradation of hazardous substances. In 2024, Yu et al. [100]. developed two porphyrin-based CMPs embedded with nanoscale zero-valent iron (Por-CMPs-1−2@nZVI) using a combined Sonogashira–Hagihara coupling and liquid-phase synthesis method. These materials exhibited both micro- and mesoporous structures. According to BET surface area analysis, the values were 181.94 and 92.63 $m^2\ g^{-1}$, respectively, with the reduced surface area attributed to pore obstruction caused by the nZVI particles. Upon visible-light exposure (≥400 nm), MB degradation efficiencies of 97% and 98% were obtained by the composites within 150 min (Figure 8L). In addition, to improve the recyclability and processability of the materials, the powder materials were converted into thin films, which resulted in a slight decrease in the photocatalytic performance (91% and 93%) (Figure 8M,N), but the recyclability of the materials was improved. This study validates the potential of superoxide and hydroxyl radicals in the photodegradation of MB and provides a new approach for doping with metal ions to modulate the photocatalytic efficiency of porous polymers.

3.6 | Selective Sulfur Oxidation

Sulfoxides, essential intermediates in pharmaceuticals, agrochemicals, and bioactive chemical production, are typically prepared through selective sulfide oxidation with molecular oxygen under sustainable conditions [102]. Still, visible-light-mediated aerobic oxidation to sulfoxides presents significant challenges in efficiency and selectivity.

Three thiazolo[5,4-*d*] thiazole (TzTz) linked CMP photocatalysts (TzTz-CMP-1,2, and 3) were prepared by Lang et al. [103] in 2021. They were designed tailor-made with π-conjugated aromatic rings of varying symmetry to manipulate their photocatalytic performance (Figure 9A). TzTz-CMP-3 was found to show the best activity toward selective sulfide oxidation under blue light exposure and the supply of atmospheric air with exceptional selectivity up to 99% (Figure 9B). The enhanced performance of TzTz-CMP-3 was achieved because of its highly symmetrical π-conjugated aromatic skeleton that was accountable for higher BET surface area than their non-symmetrically related versions. This structural feature enables more efficient conversion of oxygen to $O_2^{\bullet-}$, thereby facilitating its involvement in the selective oxidation process [104]. In 2024, Lang et al. [105]. developed two CMP-based photocatalysts incorporating TzTz linkers and investigated the impact of molecular symmetry on their performance. Among them, Py(4)-TzTz-CMP, featuring D2h symmetry, demonstrated superior optoelectronic characteristics compared to Py(2)-TzTz-CMP, which utilizes C_2-symmetric pyrene units. Under green light irradiation, Py(4)-TzTz-CMP achieved efficient conversion of sulfides to sulfoxides (Figure 9C). The work illustrates how structural symmetry in CMPs significantly influences photocatalytic efficiency and product selectivity, particularly for highvalue organic compounds.

Photocatalytic performance of materials is significantly influenced by their components of molecular construction, and π-conjugated extended structures have a tendency to facilitate faster electron movement. In this work, the electron-rich and coplanar subunit of benzotrithiophene (BTT) has attracted widespread interest. In 2024, BTT-PDAN-CMP and BTT-PDA-COF were designed and prepared by Lang et al. [106] using BTT as the core structural building block and tethered by vinylene and imine linkages, respectively (Figure 9D). Even though BTT-PDA-COF is a crystalline covalent organic framework (COF), the amorphous BTT-PDAN-CMP shows higher optoelectron performance largely due to faster electron movement facilitated by vinyl connecting linkages. For selective aerobic oxidation of sulfide applications, BTT-PDAN-CMP was found to be more efficient than its crystalline analogue.

When placed under green light exposure, the system permitted the development of reactive species of oxygen like $O_2^{\bullet-}$ and singlet oxygen ($^1O_2$), and it effected highly selective sulfide conversion to sulfoxides. Moreover, the robust framework of BTT-PDAN-CMP permitted it high recyclability and general application toward green-light-induced sulfur oxidation reactions.

Reactive oxygen species (ROS) are key regulators in determining the mechanisms and final products of redox reactions. However, the precise quantitative structure-activity relationship between photocatalyst design and the selective generation of ROS remains poorly understood. The generation of ROS is mainly due to differences in exciton processes, and for polymer photocatalysts, tunable molecular oxygen activation processes have rarely been reported without involving transition metal sites [110]. Therefore,

27662098, 2026, 2, Downloaded from https://onlinelibrary.wiley.com/doi/10.1002/EXP.20240487 by CochraneChina, Wiley Online Library on [08/06/2026]. See the Terms and Conditions (https://onlinelibrary.wiley.com/terms-and-conditions) on Wiley Online Library for rules of use; OA articles are governed by the applicable Creative Commons License

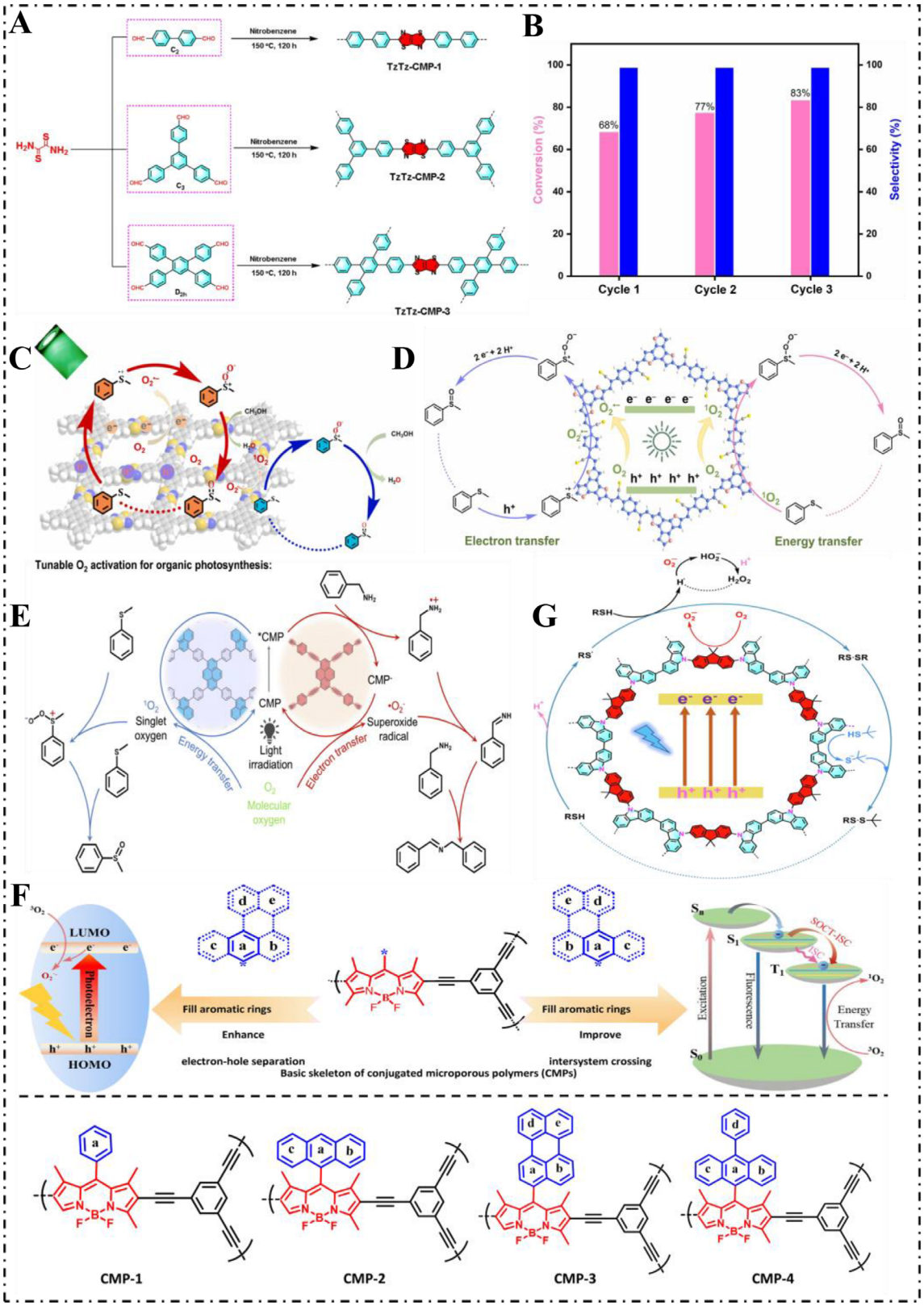


FIGURE 9 | (A) The synthesis of the three TzTz-linked CMPs. (B) Cyclic assay for the selective generation of sulfoxide by TzTz-CMP-3. Reproduced with permission [103]. Copyright 2021, Elsevier Ltd. (C) The plausible mechanism of Py(4)-TzTz-CMP photocatalysis. Reproduced with permission [105]. Copyright 2023, Elsevier Ltd. (D) Schematic of selective sulfur oxidation of BTT-PDAN-CMP photocatalyst with $O_2^{\bullet-}$ and $^1O_2$ under green light drive. Reproduced with permission [106]. Copyright 2024, Elsevier Ltd. (E) The mechanism of the photocatalytic aerobic oxidation reactions. Reproduced with permission [107]. Copyright 2021, Elsevier Ltd. (F) The design principles of PAHs-modified CMPs and the structure of CMP1–4. Reproduced with permission [108]. Copyright 2021, Wiley-VCH. (G) The possible mechanism of blue light-induced oxidation of thiols to disulfides with oxygen on MFC-CMP. Reproduced with permission [109]. Copyright 2022, Elsevier Ltd.

27662098, 2026, 2, Downloaded from https://onlinelibrary.wiley.com/doi/10.1002/EXP.20240487 by CochraneChina, Wiley Online Library on [08/06/2026]. See the Terms and Conditions (https://onlinelibrary.wiley.com/terms-and-conditions) on Wiley Online Library for rules of use; OA articles are governed by the applicable Creative Commons License

it is challenging to rationally design advanced photocatalysts to modulate ROS. In 2022, Wang et al. [107] found that ROS generation can be switched by modification of metal-free CMP, verifying for the first time the polymer-conjugated (alkyl bridge) induced controllable molecular oxygen activation introduced in non-metal-CMPs (CMP-A, CMP-D). CMP-A facilitates ICT to oxygens through the incorporation of an alkyne bridge and leads to $O_2^{\bullet-}$ formation. However, CMP-D lacking the alkyne linkage, facilitates the surface accumulation and diffusion of photo-excited carriers and preferentially leads to $^1O_2$ formation (Figure 9E). The dehydrogenation of benzamide and the oxidation of thioether were realized by two CMPs under light drive, and the catalyst loading could be reduced to 0.1% and 1%, respectively, which provided insights for the rational design of various heterogeneous organic photocatalyst CMPs.

The efficiency of photosensitization is strongly linked to a material's light absorption and capabilities and its ability to transfer energy or electrons—core processes also found in natural photosynthesis. While heavy metal atoms have traditionally been used to improve photosensitization, this strategy comes with notable drawbacks. In 2021, Guo et al. [108]. advanced the photosensitization performance of CMPs by integrating polycyclic aromatic hydrocarbons (PAHs) into their structures. By using a bottom-up synthetic method, benzo[a]anthracene and biphenyl subunits were integrated into Bodipy-based CMPs by Guo to prepare CMP-2, CMP-3 and CMP-4. Compared to CMP-1, both of these new CMPs had reduced fluorescence and higher effective intersystem crossing (ISC) or larger electron–hole cleavage, It was found that the yield of methylphenyl sulfoxide was 92% for the photocatalytic reaction of CMP-2 and was markedly higher than the 32% yield of the reaction of CMP-1 (Figure 9F). These results show that it is feasible to integrate PAHs into the backbone of CMPs and open up new channels of charge transmission and boost ISC and endow effective photocatalytic electron and energy transmission processes.

Disulfide bonds are commonly found in naturally occurring bioactive compounds, including peptides, making the selective oxidation of thiols an important chemical transformation. The formation of disulfides has gained significant attention in pharmaceutical and chemical industries [111]. Utilizing porous conjugated polymers as photocatalysts with molecular oxygen as the oxidant presents an effective approach for thiol oxidation. Nevertheless, this reaction generally depends on the combined effect of a Brønsted base and a photocatalyst to proceed efficiently. Carbazole, due to its Brønsted basicity, can assist in facilitating disulfide formation, making it a promising structural component for integrating both catalytic functions into CMPs for efficient and selective thiol-to-disulfide oxidation [112]. In 2022, Lang et al. [109]. utilized two precursors—9,9′-(9,9-dimethyl-9*H*-fluorene-2,7-diyl)bis(9*H*-carbazole) (MFC) and 9,9′-(9,9-difluoro-9*H*-fluorene-2,7-diyl) bis (9*H*-carbazole) (FFC)—to synthesize MFC-CMP and FFC-CMP via oxidative polymerization with ferric chloride. The CMPs demonstrated the ability to convert O_2 into $O_2^{\bullet-}$ radicals, which facilitated the blue-light-driven selective oxidation of thiols to symmetrical disulfides. Mechanistic studies indicated that upon blue light exposure, photoinduced electrons were transferred from the carbazole units to the fluorene moiety in MFC-CMP, facilitating the activation of oxygen into $O_2^{\bullet-}$ species. Concurrently, thiol groups adsorbed on the MFC-CMP released protons and were converted into sulfur-centered free radicals ($RS^{\bullet}$), which then combined with other thiols to form corresponding symmetric disulfide compounds, while hydrogen radicals ($H^{\bullet}$) were simultaneously released. Subsequently, $H^{\bullet}$ and $O_2^{\bullet-}$ combine to form perhydroxy anion (HO_2^-), which is further consumed to convert the resulting H^+ into hydrogen peroxide (H_2O_2) (Figure 9G). The H^+ of tert-butyl thiol is absorbed by carbazole of MFC-CMP, producing anions. Asymmetric disulfides were produced through an S_N2-type nucleophilic substitution reaction, in which symmetric disulfides reacted with tert-butyl thiol anions. This study emphasizes the potential of integrating synergistic photocatalytic functions into CMPs to enable diverse chemical transformations.

3.7 | Synthesis of Benzoheterocyclic Compounds

Benzimidazole rings are ubiquitous within biologically active molecules and are vital intermediates and co-ligands that are employed within organic synthesis [113]. Traditional routes of syntheses of benzimidazole derivatives favor harsh conditions and are therefore quite undesirable. Compared with these traditional routes of syntheses, photocatalytic synthesis is a cleaner, softer, and environmentally friendly alternative [114]. In 2020, An et al. [33]. employed the bottom-up approach synthesizing two of their CMPs—BTP-CMP and TBTP-CMP—with dithiophene and thiophene components embedded, both of which were endowed with exceptional photocatalytic capacity for synthesizing benzimidazole. The electron-rich thiophene moieties within the π conjugated TP-CMPs contributed to beneficial band structures and boosted photochemical activity. Through the use of BTP-CMP under illumination of visible light, more than 91% yield of benzimidazole was achieved. It was found to possess exceptional reusability (i.e., 15 cycles with yields of 96%–98%) and robustness and was a steady and highly effective heterogeneous photocatalyst. In 2021, Liu et al. [115]. prepared three conjugated porous polymers—BTT-CMP1, BTT-CMP2, and BTT-CMP3—constructed from benzo[1,2-b:3,4-b′:5,6-b″]trithiophene (BTT) units. They tuned the linkers between BTT moieties and achieved bandgap engineering and tailoring of the energy levels and optoelectronical features of the materials (Figure 10A). BTT-CMP2 was found to exhibit the optimum light-activated charge generation, transfer, and separation and produce $O_2^{\bullet-}$ best. This material was proven to exhibit remarkable catalytic capacity for benzimidazole synthesis under illumination.

Boron-based chromophores, being electron-deficient, are viewed as effective photocatalyst candidates because of their remarkable electron-accepting abilities, high light absorption, strong fluorescence, and elevated quantum efficiencies. In 2022, Gong et al. [116]. incorporated boron containing dyes units into the framework of CMPs to synthesize two novel materials: Cz-BF_2-CMP and Cz-BPh_2-CMP (Figure 10B). Through strong donor–acceptor interactions between carbazole and boron-based dyes, these CMPs enhanced interfacial charge transfer and separation of photogenerated carriers. Thus, Cz-BF_2-CMP displayed excellent photocatalytic properties, particularly in water-based green synthesis of benzimidazoles and aerobic thioether oxidation in ethanol. In a similar context, 2,6-dimethyl-4*H*-pyran-4-ylidene-malononitrile (DCM), known for its excellent chemical stability and strong electron-accepting nature, has gained attention as

27662098, 2026, 2, Downloaded from https://onlinelibrary.wiley.com/doi/10.1002/EXP.20240487 by CochraneChina, Wiley Online Library on [08/06/2026]. See the Terms and Conditions (https://onlinelibrary.wiley.com/terms-and-conditions) on Wiley Online Library for rules of use; OA articles are governed by the applicable Creative Commons License

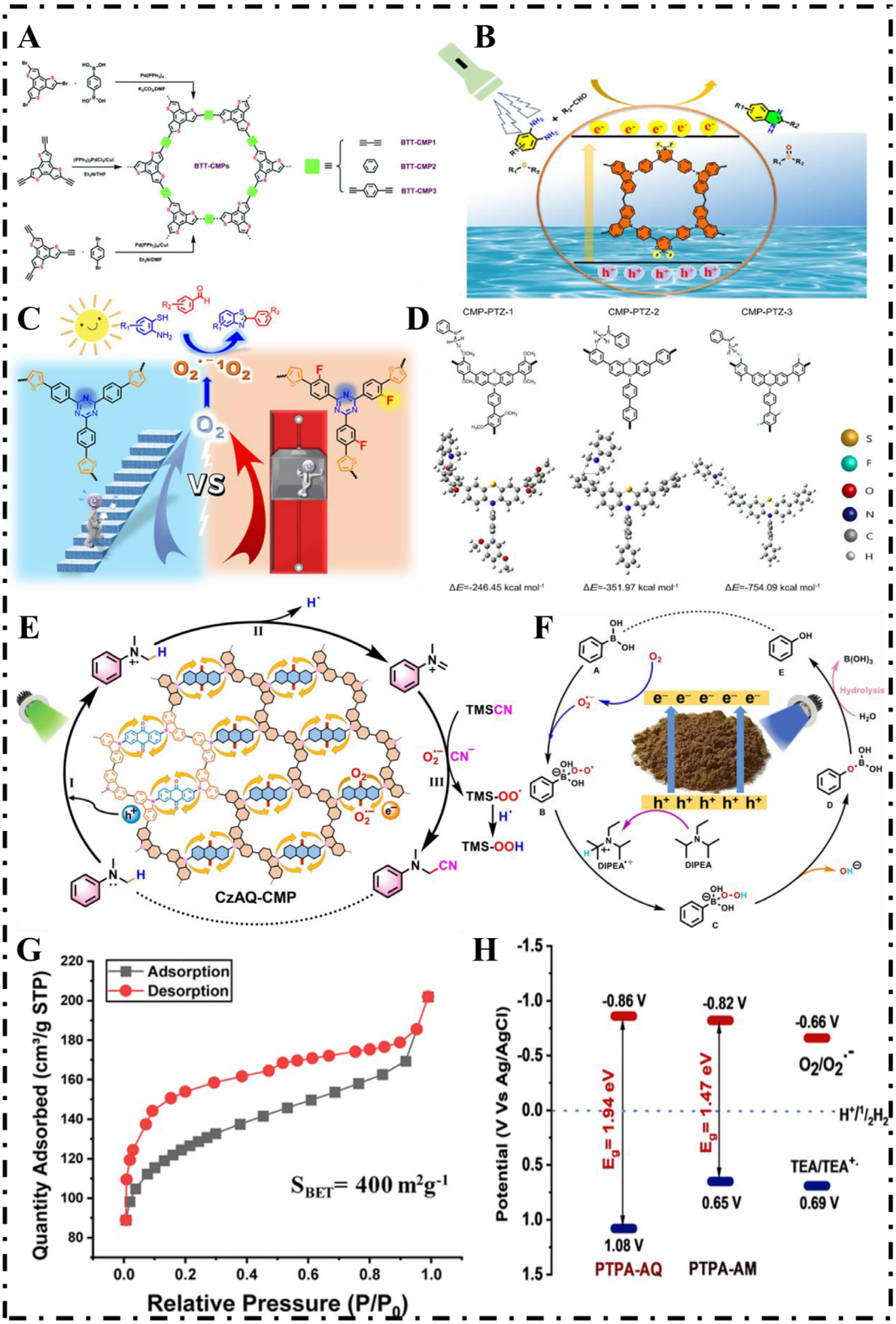


FIGURE 10 | (A) Syntheses of BTT-CMPs. Reproduced with permission [115]. Copyright 2020, Royal Society of Chemistry. (B) Catalytic mechanism diagram of Cz-BF_2-CMP. Reproduced under the terms of the Creative Commons CC-BY license [116]. Copyright 2022, The Authors. (C) Photocatalytic process of CMPs. Reproduced with permission [117]. Copyright 2023, American Chemical Society. (D) Optimized structures of hydrogen-bonded complexes. Reproduced with permission [118]. Copyright 2020, Elsevier Ltd. (E) A preliminary mechanism for the CzAQ-CMP catalyzed aerobic oxidative cyanidation of *N*,*N*-dimethylaniline. Reproduced with permission [119]. Copyright 2023, Elsevier Ltd. (F) Possible mechanism of EFC-CMP aerobic hydroxylation of phenylboronic acid to phenol. Reproduced with permission [120]. Copyright 2022, Elsevier Ltd. (G) Nitrogen adsorption-desorption isotherms of PTPA-AQ at 77 K. (H) HOMO–LUMO positions of the D–A CMPs. Reproduced with permission [121]. Copyright 2023, Royal Society of Chemistry.

27662098, 2026, 2, Downloaded from https://onlinelibrary.wiley.com/doi/10.1002/EXP.20240487 by CochraneChina, Wiley Online Library on [08/06/2026]. See the Terms and Conditions (https://onlinelibrary.wiley.com/terms-and-conditions) on Wiley Online Library for rules of use; OA articles are governed by the applicable Creative Commons License

a fluorescent chromophore. It is widely applied in developing narrow-bandgap photoactive CMPs due to its favorable optoelectronic properties. In 2024, Liu et al. [48]. successfully synthesized two novel sp^2 carbon bonded DCM-CMPs (DCM-CMP1 and DCM-CMP2) by Knoevenagel reaction using DCM and aromatic polyaldehydes as monomers, which have wide photoadsorption, good durability, and excellent optoelectronic properties. Notably, DCM-CMP2 serves as a metal-free photocatalyst that demonstrates strong catalytic efficiency, wide substrate tolerance, and outstanding recyclability in the visible-light synthesis of benzimidazoles. This research effectively expands the utility of CMPs as heterogeneous photocatalysts, and paves the way for developing advanced solid-state photocatalysts derived from luminescent dye-based architectures.

Benzothiazole and its derivatives constitute a significant family of heterocycles found abundantly in nature and utilized largely in pharmaceuticals, agriculture, and industry. The photocatalytic synthesis of these molecules is of significant environmental value [122]. In 2023, Zhang et al. [117]. developed two D–A type CMPs, namely CMP-Th-Ph and CMP-Th-Ph-F) incorporating triazine units. By integrating fluorine atoms into the CMP framework, they successfully created dual active sites involving both fluorine and nitrogen atoms and enhanced oxygen adsorption and electron and energy transfer processes (Figure 10C). These polymers selectively produced $O_2^{\bullet-}$ and $^1O_2$ Under green light illumination. Under photocatalytic conditions, 2-aminothiophenol and benzaldehyde were oxidized and transformed to benzothiazole intermediates. This study not only introduces a novel approach for activating oxygen through organic semiconductor-based photocatalysts but also contributes to advancing exciton manipulation strategies aimed at optimizing photocatalytic performance.

3.8 | Oxidative Cyanide of Tertiary Amines

The oxidation of tertiary amines is a fundamental biochemical transformation that plays a crucial role in biological systems. As key precursors to nitrogen-containing compounds, tertiary amines have garnered significant interest in organic synthesis. Traditionally, their direct cyanation has required metal-based catalysts under elevated temperatures, and there have been limited studies using multiphase photocatalytic systems for this purpose. With their characteristic physicochemical advantages, CMPs hold significant potential for use in photocatalytic oxidative cyanation of tertiary amines [123]. In 2021, Zhang et al. [118]. introduced a series of PTZ-CMPs as fully organic photocatalysts capable of facilitating this reaction under visible light and ambient conditions. Through altering electron-donating and electron-withdrawing groups on the monomers, the researchers successfully regulated charge separation and enhanced photocatalytic efficiency. Notably, CMP-PTZ-3, which features fluorine substituents, exhibits excellent catalytic activity and recyclability—attributed to the formation of C-F···H-X interactions between the polymer and substrate that enhance reaction efficiency. DFT calculations revealed that CMP-PTZ-3 had the strongest interaction energy (−754.09 kcal mol^{-1}), compared to CMP-PTZ-2 (−351.97 kcal mol^{-1}) and CMP-PTZ-1 (−246.45 kcal mol^{-1}), suggesting stronger hydrogen bonding (Figure 10D). This work introduces a novel class of metal-free multiphase photocatalysts and presents a refined molecular design approach for CMP-based photocatalysis.

To investigate the synergistic interaction between electron-deficient AQ and electron-rich carbazole for facilitating continuous electron flow in CMPs and enhancing photocatalytic efficiency, Lang et al. [119] synthesized a CMP named CzAQ-CMP in 2023. This material was obtained through homogeneous polymerization of a monomer (CzAQ) composed of carbazole (donors) and AQ (acceptor). Theoretical calculations validated that the AQ units within the photocatalyst promote electron transfer to molecular oxygen, resulting in the formation of $O_2^{\bullet-}$. The porous architecture of CzAQ-CMP plays a vital role in enhancing its photocatalytic performance for aerobic oxidative cyanation of *N,N*-dimethylaniline in methanol (Figure 10E). In addition, in acetic acid medium, it catalyzes oxidative cyanation of different primary amines with excellent selectivity of up to 99%. This study introduces a novel approach and catalyst system for the application of CMPs in environmentally sustainable organic synthesis.

3.9 | Hydroxylation of Aryl Boronic Acids

Phenols and their substitutes are common in various natural products and intermediates and are highly significant parts of polymers, pharmaceuticals, agricultural chemicals, and other bioactive entities. It is nevertheless still a challenging task to achieve direct hydroxylation of aromatic C-H bonds. On the other hand, it is easier to achieve hydroxylation when pre-functionalized aromatic substrates such as aryl halides or phenylboronic acids are utilized based on more accessible reactive centers. Visible photocatalysis of great interest in the selective production of phenol from aryl halides or aryl boronic acids using oxygen as an oxidant. Among the various ROSs, $O_2^{\bullet-}$ is particularly well-suited for the selective aerobic hydroxylation of aryl boronic acids to produce phenols. In 2022, Lang et al. [120]. developed two carbazole-based CMPs (TCB-CMP and EFC-CMP) via C-C coupling polymerization using 1,3,5-tri(9*H*-carbazole-9-yl)benzene (TCB) and 9,9′-(9,9-diethyl-9*H*-fluorene-2,7-diyl)bis(9*H*-carbazole) (EFC) as building blocks. Under blue light irradiation and using *N*,*N*′-diisopropylethylamine (DIPEA) as a hole scavenger, both CMPs were capable of catalyzing the aerobic hydroxylation of phenylboronic acid in ethanol (Figure 10F). EFC-CMP outperformed TCB-CMP in catalytic activity, which is likely attributed to its greater efficiency in reducing oxygen to $O_2^{\bullet-}$, thereby enabling high-yield hydroxylation of various phenylboronic acid substrates. In 2023, Soumitra et al. [121]. synthesized two new D–A CMPs, PTPA-AQ, and PTPA-AM, using Suzuki–Miyaura cross-coupling for visible light-driven oxidative hydroxylation of phenyl boronic acids. PTPA-AQ exhibited a higher BET surface area of 400 m^2 g^{-1} (Figure 10G), an optimal band gap of 1.94 eV and favorable HOMO-LUMO energy levels, resulting in exceptional catalytic performance with phenol yield reaching 96% (Figure 10H).

3.10 | Oxidative Coupling of Amines

Imines are very useful organic intermediates which are utilized widely in pharmaceuticals and related industries. Oxidation of amines using photocatalysts is a green and environmentally

27662098, 2026, 2, Downloaded from https://onlinelibrary.wiley.com/doi/10.1002/EXP.20240487 by CochraneChina, Wiley Online Library on [08/06/2026]. See the Terms and Conditions (https://onlinelibrary.wiley.com/terms-and-conditions) on Wiley Online Library for rules of use; OA articles are governed by the applicable Creative Commons License

friendly approach of synthesizing imines where the reaction can occur under noncontaminating and mild conditions. In 2020, Zhou et al. [124]. prepared carbazoporphyrin based CMPs (TCPP-CMP) by simple $FeCl_3$-catalyzed oxidative polymerization. Under natural light, TCPP-CMP is able to promote the aerobic oxidation of benzylamine and thioanisole with high conversion and selectivity. In 2021, Lang et al. [125]. synthesized two fluorenyl-based CMPs—MFC[9,9′-(9,9-dimethyl-9*H*-fluorene-2,7-diyl)bis(9*H*-carbazole)]-CMP, FFC[9,9′-(9,9-difluoro-9*H*-fluorene-2,7-diyl)bis(9*H*-carbazole)]-CMP—via $FeCl_3$-catalyzed oxidative polymerization (Figure 11A). Variation at the 9-position of the fluorene methylene bridge enabled fine control over CMP photocatalytic properties. MFC-CMP, in particular, possessed a large BET surface area and efficient electron-hole separation, delivering outstanding amine oxidation activity under blue light.

Borane dyes are new fluorescent boron complexes of the NˆBˆO coordination motif and are promising building components of CMPs. Having disc-like π-conjugated structure with multicenter boron often results in their higher photophysical performance than ordinary dye molecules and hence are very desired building constituents of complex photocatalytic materials. In 2021, Gong's team [126] designed and successfully prepared a new boronalkyl CMP (TDFB-TEB). In comparison to the borane-free TCT-TEB, TDFB-TEB feature a narrower band gap of 1.94 eV (Figure 11B), and demonstrates excellent catalytic performance in both sulfide and primary amine oxidation reactions, achieving high conversion rates of up to 90% along with strong reusability (Figure 11C,D). In 2022, Lang's group designed six CMPs based on D–A [127] (Py-DTDO-2 and Py-DTDO-4) (Figure 11E) and D–π–A (TzTz-CMP-Be, TzTz-CMP-Py [129], TzTz-Bz and TzTz-BTT [128]) (Figure 11F), respectively. All of these materials exhibited excellent photocatalytic performance, and the combined findings provide meaningful guidance for the tailored development of high-performance CMPs suited to a wide range of photocatalytic applications.

Owing to its electron-rich character, strong charge transport ability, ease of chemical modification, and rigid π-conjugated framework, thiophene is extensively employed as an electron donor or π-bridge in CMP synthesis. In 2023, Zhang et al. [130]. reported the creation of two thiophene-fused CMPs—TT-Py-CMP and DTT-Py-CMP—by coupling thieno[3,2-*b*] thiophene (TT) and dithieno[3,2-*b*:2′,3′-*d*] thiophene (DTT) with 1,3,6,8-tetrabromopyrene. Results from DFT calculations confirmed that extending the π-system from TT to DTT strengthened visible-light absorption and improved charge separation. Accordingly, the CMPs displayed superior catalytic activity in the selective aerobic oxidation of amines to imines. Notably, under red LED illumination, DTT-Py-CMP achieved a higher conversion rate of benzylamine compared to TT-Py-CMP.

The effectiveness of photocatalysts is often hindered by inefficient light utilization and limited substrate access to active sites. As a result, hollow CMPs have gained considerable attention due to their potential to improve catalytic performance and enable atom-economical catalyst design through morphological tuning. [131, 132] In 2024, Cai et al. [31]. synthesized CMPs incorporating BTD units onto SiO_2 microspheres surfaces via a Sonogashira–Hagihara coupling reaction, After removing the silica core, hollow structures—*h*PorSTZ and *h*PorDTZ—were obtained (Figure 11G). Their high surface area and modifiable surface active centers significantly boosted catalytic activity in oxidative coupling reactions of diverse primary amines. Compared to their solid counterpart (cPorDTZ), the hollow CMPs demonstrated superior reusability (over five cycles) and rapid conversion rates exceeding 90%. Xu et al. [32]. utilized dibromopyrazine and 1,3,5-triacetylene benzene to synthesize a series of pyrazine-based hollow spherical CMPs—H-PyB-1 to H-PyB-4—via a templating strategy, yielding structures with diameters between 630 nm and 200 nm. The confined polymerization process enhanced π-conjugation, improved electrical conductivity (Figure 11H), reduced band gaps (Figure 11I), and enhanced optoelectronic properties. Notably, the smallest variant, H-PyB-4, achieved outstanding performance in photocatalytic amine oxidation, reaching a yield of approximately 113 mmol g^{-1} h^{-1} with near 100% selectivity for the resulting imine (Figures 11J and 11K). The study proposes a novel size-limited synthesis method to design advanced organic photocatalysts, paving the way for durable, efficient, and reusable metalfree CMPs applicable to a wide range of transformations.

3.11 | Other Reactions

Light-driven organic transformations, for example, photocatalytic reductive dehalogenation, can constitute a very promising avenue toward green chemical syntheses. In 2023, Tang et al. [133]. developed an effective strategy for achieving highly efficient multiphase photocatalytic dehalogenation under mild conditions by modulating the exciton binding energy through variations in D–A structural frameworks. Among the materials studied, CMP-CSU11, featuring the most optimized D–A architecture and consequently the lowest exciton binding energy, exhibited exceptional photocatalytic dehalogenation performance—achieving over 99% efficiency in approximately 50 min. It was discovered to exhibit high substrate compatibility (14 diverse substrates) and was very highly reusable and outperformed many of the available photocatalysts.

In 2023, Xu et al. [132]. constructed carbazole-based hollow CMP spheres (H-CTB) by sacrificial template method. Compared with the conventional CMP (P-CTB), the hollow-structure analogue (H-CTB) exhibited higher physicochemical properties. H-CTB, upon exposure to blue light, efficiently oxidized phenylethanol, producing more than 1 mmol of benzaldehyde within 4.5 h and attaining a peak rate of 9 mmol h^{-1} g^{-1}, surpassing conventional CMP performance. The hollow design also facilitated oxidation reactions of other aromatic alcohols.

4 | Summary and Outlook

Since their first demonstration in 2012, CMP-based materials have made significant advancements in photocatalysis, showing great potential for converting photon energy into sustainable chemicals. CMPs, a subclass of COFs, constitute a new category of porous materials that integrate multiple beneficial features. These include extended π-conjugated, outstanding optical and electronic characteristics, large surface area, intrinsic porosity, robust structural stability, tunable architectures, efficient

27662098, 2026, 2, Downloaded from https://onlinelibrary.wiley.com/doi/10.1002/EXP.20240487 by CochraneChina, Wiley Online Library on [08/06/2026]. See the Terms and Conditions (https://onlinelibrary.wiley.com/terms-and-conditions) on Wiley Online Library for rules of use; OA articles are governed by the applicable Creative Commons License

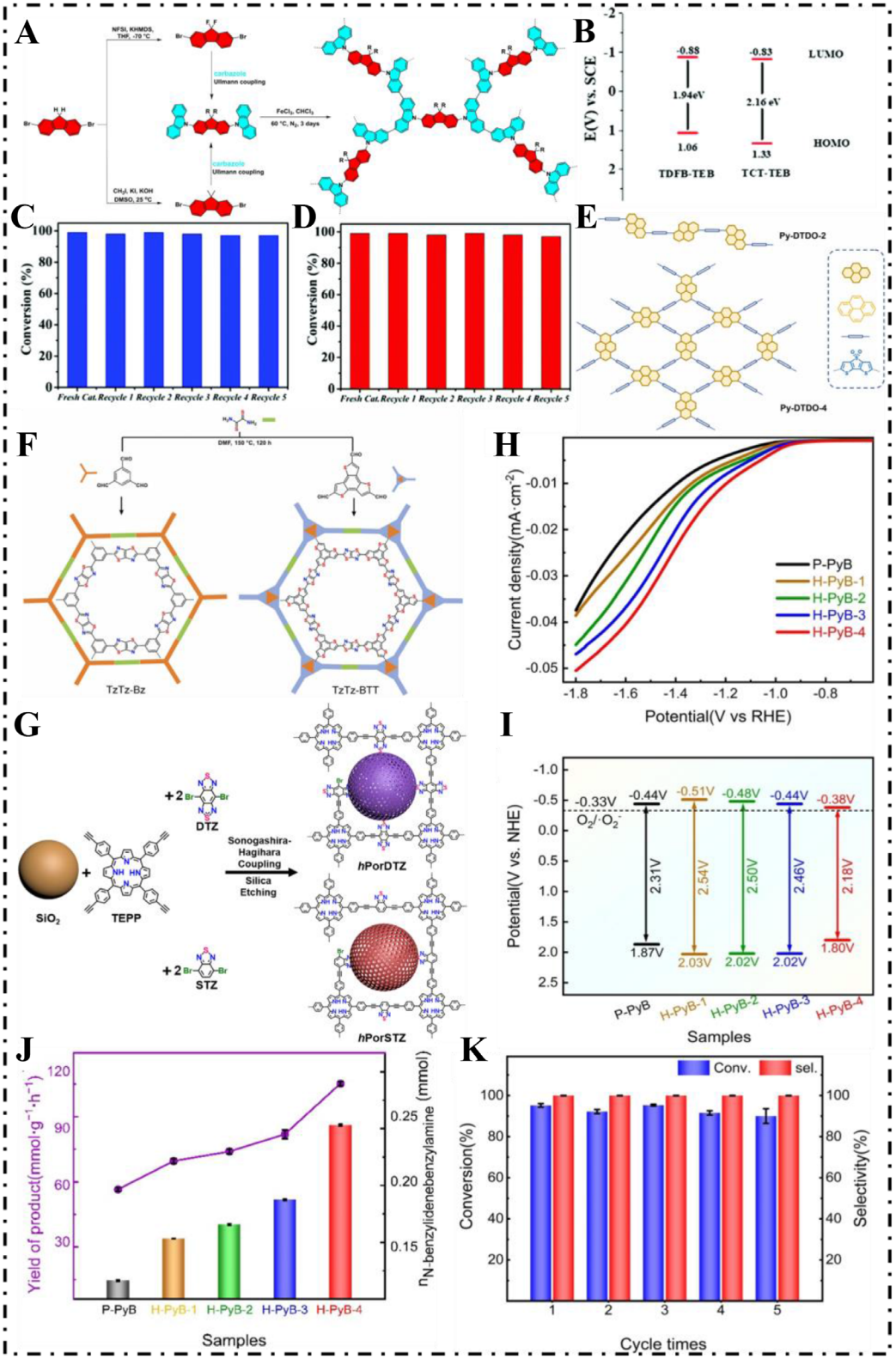


FIGURE 11 | (A) Schematic of the design and preparation of two CMPs derived from fluorene. Reproduced with permission [125]. Copyright 2020, Elsevier Ltd. (B) Energy band diagrams of TCT-TEB and TDFB-TEB. (C, D) Assessment of the reusability of TDFB-TEB in (C) oxidation of sulfides and (D) coupling of amines. Reproduced with permission [126]. Copyright 2021, Royal Society of Chemistry. (E) Schematic illustration for Py-DTDO-2 and Py-DTDO-4. Reproduced with permission [127]. Copyright 2022, Elsevier Ltd. (F) Synthetic routes of TzTz-Bz and TzTz-BTT. Reproduced with permission [128]. Copyright 2023, Elsevier Ltd. (G) Synthetic routes for *h*PorDTZ and *h*PorSTZ microspheres. Reproduced with permission [31]. Copyright 2023, Wiley-VCH. (H) The linear sweep voltammetry curves. (I) The HOMO and LUMO energy levels derived from their optical bandgaps and cyclic voltammetry results. (J) Comparison of the yield of corresponding *N*-benzylidene benzylamine of different photocatalysts. (K) Recycle experiments over H-PyB-4 CMPs. Reproduced with permission [32]. Copyright 2024, Elsevier Ltd.

27662098, 2026, 2, Downloaded from https://onlinelibrary.wiley.com/doi/10.1002/EXP.20240487 by CochraneChina, Wiley Online Library on [08/06/2026]. See the Terms and Conditions (https://onlinelibrary.wiley.com/terms-and-conditions) on Wiley Online Library for rules of use; OA articles are governed by the applicable Creative Commons License

visible-light absorption, and excellent charge mobility—all while being metal-free. Due to these qualities, CMPs have become a highly adaptable platform for photochemical applications, enabling diverse processes such as energy harvesting, environmental remediation, and various organic transformations.

Future developments in CMP-based photocatalysts should focus on several key strategies to enhance their performance. One crucial area is the reduction of carrier recombination rates. This can be achieved through the construction of heterojunctions, a strategy proven effective in promoting exciton dissociation in organic semiconducting materials, as demonstrated in organic solar cells. Similarly, the integration of other semiconducting materials into CMPs can improve charge generation and photocatalytic activity. Moreover, doping CMPs with heteroatoms, such as nitrogen, oxygen, phosphorus, or sulfur allows for precise tuning of their electronic band structures, extend light absorption and promoting more efficient charge carrier separation. Surface functionalization—either through the attachment of targeted functional groups or the incorporation of metal nanoparticles—can further enhance their surface properties, adsorption capacity, and catalytic activity. The incorporation of cocatalysts, such as noble metal nanoparticles or transition metal compounds, can reduce activation energy, improving reaction rates and selectivity in photocatalytic processes.

Expanding the visible light absorption range is another key strategy for enhancing CMP photocatalytic performance. This can be achieved by incorporating chromophores or dye molecules with strong visible light absorption properties, which absorb light and transfer the energy to the polymer's conjugated backbone, improving its ability to utilize visible light. Additionally, adjusting the polymer skeleton structure by modifying monomer composition and polymerization methods can influence electron delocalization and the band structure, broadening the light absorption range.

An effective strategy to boost catalytic efficiency involve increasing the accessibility of active sites, Template-assisted synthesis enables the fabrication of CMPs with customized morphologies and pore structures, thereby improving the exposure and accessibility of catalytic active sites. In addition, post-synthetic modifications—such as acid, base, or redox treatments—can eliminate surface impurities and excess polymer segments, further revealing internal active sites and enhancing catalytic efficiency.

The continuous development of CMPs in photocatalysis positions them as an emerging and versatile technology for light-driven reactions. With ongoing research focused on optimizing structural design, enhancing light absorption, and improving charge carrier dynamics, CMP-based photocatalysts hold great promise for addressing global challenges in energy production, environmental remediation, and sustainable chemical synthesis.

Author Contributions

Dun Zhou wrote the manuscript; Kongqing Zhang organized and collected the literature; Xiaobai Li and Hongwei Ma: project management, supervision, fund acquisition, and writing; Yongpeng Liu and Liang Yao: proofreading and supervision; this paper was jointly revised by all authors.

Acknowledgments

This work was financially supported by National Key Research and Development Program of China (2023YFF1304903), National Natural Science Foundation of China (22576031, 22374017), Fundamental Research Funds for the Central Universities (2572025JT07), the Natural Science Foundation of Heilongjiang Province (2024ZXDXC28).

Ethics Statement

This thesis does not deal with any ethical issues.

Conflicts of Interest

The authors declare no conflicts of interest.

Data Availability Statement

The data that support the findings of this study are available from the corresponding author upon reasonable request.

References

1. D. Shindell and C. J. Smith, "Climate and Air-Quality Benefits of a Realistic Phase-Out of Fossil Fuels," *Nature* 573 (2019): 408–411, https://doi.org/10.1038/s41586-019-1554-z.

2. D. Tong, Q. Zhang, Y. Zheng, et al., "Committed Emissions From Existing Energy Infrastructure Jeopardize 1.5 °C Climate Target," *Nature* 572 (2019): 373–377, https://doi.org/10.1038/s41586-019-1364-3.

3. C. Kemfert, F. Präger, I. Braunger, F. M. Hoffart, and H. Brauers, "The Expansion of Natural Gas Infrastructure Puts Energy Transitions at Risk," *Nature Energy* 7 (2022): 582–587, https://doi.org/10.1038/s41560-022-01060-3.

4. A. J. Carrillo, J. González-Aguilar, M. Romero, and J. M. Coronado, "Solar Energy on Demand: A Review on High Temperature Thermochemical Heat Storage Systems and Materials," *Chemical Reviews* 119 (2019): 4777–4816, https://doi.org/10.1021/acs.chemrev.8b00315.

5. Z. Wang, C. Li, and K. Domen, "Recent Developments in Heterogeneous Photocatalysts for Solar-Driven Overall Water Splitting," *Chemical Society Reviews* 48 (2019): 2109–2125, https://doi.org/10.1039/C8CS00542G.

6. Y. Wang, H. Suzuki, J. Xie, et al., "Mimicking Natural Photosynthesis: Solar to Renewable H_2 Fuel Synthesis by Z-Scheme Water Splitting Systems," *Chemical Reviews* 118 (2018): 5201–5241, https://doi.org/10.1021/acs.chemrev.7b00286.

7. Y. Liu, C. Pulignani, S. Webb, et al., "Electrostatic [FeFe]-Hydrogenase–Carbon Nitride Assemblies for Efficient Solar Hydrogen Production," *Chemical Science* 15 (2024): 6088–6094, https://doi.org/10.1039/D4SC00640B.

8. Y. Liu, S. Webb, P. Moreno-Garcia, et al., "Facile Functionalization of Carbon Electrodes for Efficient Electroenzymatic Hydrogen Production," *JACS Au* 3 (2023): 124–130, https://doi.org/10.1021/jacsau.2c00551.

9. D. Gust and T. A. Moore, "Mimicking Photosynthesis," *Science* 244, no. 4900 (1989): 35–41.

10. F. Wen and C. Li, "Hybrid Artificial Photosynthetic Systems Comprising Semiconductors as Light Harvesters and Biomimetic Complexes as Molecular Cocatalysts," *Accounts of Chemical Research* 46, no. 11 (2013): 2355–2364.

11. A. Fujishima and K. Honda, "Electrochemical Photolysis of Water at a Semiconductor Electrode," *Nature* 238 (1972): 37–38.

12. E. Pastor, M. Sachs, S. Selim, J. R. Durrant, A. A. Bakulin, and A. Walsh, "Electronic Defects in Metal Oxide Photocatalysts," *Nature*

27662098, 2026, 2, Downloaded from https://onlinelibrary.wiley.com/doi/10.1002/EXP.20240487 by CochraneChina, Wiley Online Library on [08/06/2026]. See the Terms and Conditions (https://onlinelibrary.wiley.com/terms-and-conditions) on Wiley Online Library for rules of use; OA articles are governed by the applicable Creative Commons License

Reviews Materials 7 (2022): 503–521, https://doi.org/10.1038/s41578-022-00433-0.

13. Y. Liu, M. Xia, D. Ren, et al., "Photoelectrochemical CO_2 Reduction at a Direct $CuInGaS_2$/Electrolyte Junction," *ACS Energy Letters* 8 (2023): 1645–1651, https://doi.org/10.1021/acsenergylett.3c00022.

14. Y. Liu, M. Bouri, L. Yao, et al., "Identifying Reactive Sites and Surface Traps in Chalcopyrite Photocathodes," *Angewandte Chemie, International Edition* 60 (2021): 23651–23655, https://doi.org/10.1002/anie.202108994.

15. S. Cao, S. Wu, X. Dong, et al., "Biosafe Saccharomyces Cerevisiae Immobilized Nanofibrous Aerogels for Integrated Lead Removal in Human Body," *Advanced Functional Materials* 33 (2023): 2215059, https://doi.org/10.1002/adfm.202215059.

16. L. Chen, T. Bi, E. Lizundia, et al., "Biomass Waste-Assisted Micro(Nano)Plastics Capture, Utilization, and Storage for Sustainable Water Remediation," *Innovation (Cambridge)* 5 (2024): 100655.

17. J.-S. M. Lee and A. I. Cooper, "Advances in Conjugated Microporous Polymers," *Chemical Reviews* 120 (2020): 2171–2214, https://doi.org/10.1021/acs.chemrev.9b00399.

18. J. X. Jiang, F. Su, A. Trewin, et al., "Conjugated Microporous Poly(Aryleneethynylene) Networks," *Angewandte Chemie, International Edition* 46 (2007): 8574–8578, https://doi.org/10.1002/anie.200701595.

19. D. Zhou, K. Zhang, S. Zou, X. Li, and H. Ma, "Conjugated Microporous Polymers: Their Synthesis and Potential Applications in Flexible Electrodes," *Journal of Materials Chemistry A* 12 (2024): 17021, https://doi.org/10.1039/D4TA02085E.

20. H. Ma, Y. Chen, X. Li, and B. Li, "Advanced Applications and Challenges of Electropolymerized Conjugated Microporous Polymer Films," *Advanced Functional Materials* 31 (2021): 2101861, https://doi.org/10.1002/adfm.202101861.

21. N. N. Vu, S. Kaliaguine, and T. O. Do, "Critical Aspects and Recent Advances in Structural Engineering of Photocatalysts for Sunlight-Driven Photocatalytic Reduction of CO_2 Into Fuels," *Advanced Functional Materials* 29 (2019), https://doi.org/10.1002/adfm.201901825.

22. C. Dai and B. Liu, "Conjugated Polymers for Visible-Light-Driven Photocatalysis," *Energy & Environmental Science* 13 (2020): 24–52, https://doi.org/10.1039/C9EE01935A.

23. A. Wieczorek, Y. Liu, H.-H. Cho, and K. Sivula, "Assessing the Charge Carrier Dynamics at Hybrid Interfaces of Organic Photoanodes for Solar Fuels," *Journal of Physical Chemistry Letters* 15 (2024): 6347–6354, https://doi.org/10.1021/acs.jpclett.4c01170.

24. F. Boudoire, Y. Liu, F. Le Formal, N. Guijarro, C. R. Lhermitte, and K. Sivula, "Spray Synthesis of $CuFeO_2$ Photocathodes and in-Operando Assessment of Charge Carrier Recombination," *Journal of Physical Chemistry C* 125 (2021): 10883–10890, https://doi.org/10.1021/acs.jpcc.1c02282.

25. Y. Liu, N. Guijarro, and K. Sivula, "Understanding Surface Recombination Processes Using Intensity-Modulated Photovoltage Spectroscopy on Hematite Photoanodes for Solar Water Splitting," *Helvetica Chimica Acta* 103 (2020): e2000064, https://doi.org/10.1002/hlca.202000064.

26. Y.-K. P. Y. Y. Li, L. S. Hu, J. W. Zheng, et al., "Photocatalytic Water Splitting by N-TiO_2 on MgO (111) With Exceptional Quantum Efficiencies at Elevated Temperatures," *Nature Communications* 10 (2019): 4421, https://doi.org/10.1038/s41467-019-12385-1.

27. M. Zhang, M. Lu, Z. L. Lang, et al., "Semiconductor/Covalent-Organic-Framework Z-Scheme Heterojunctions for Artificial Photosynthesis," *Angewandte Chemie, International Edition* 59 (2020): 6500–6506, https://doi.org/10.1002/anie.202000929.

28. L. W. Yang Bai, B. J. Slater, M. A. Zwijnenburg, R. S. Sprick, and A. I. Cooper, "Accelerated Discovery of Organic Polymer Photocatalysts for Hydrogen Evolution From Water Through the Integration of Experiment and Theory," *Journal of the American Chemical Society* 141 (2019): 9063–9071.

29. Z. Tang, S. Xu, N. Yin, et al., "Reaction Site Designation by Intramolecular Electric Field in Tröger's-Base-Derived Conjugated Microporous Polymer for Near-Unity Selectivity of CO_2 Photoconversion," *Advanced Materials* 35 (2023): 2210693, https://doi.org/10.1002/adma.202210693.

30. W. Wu, M. Chen, Y. Deng, et al., "Fabrication of Novel Fluorene Incorporated Conjugated Microporous Polymer Nanotubes for Visible-Light CO_2 Reduction With Water Vapor," *Polymer Chemistry* 14 (2023): 4679–4684, https://doi.org/10.1039/D3PY00493G.

31. S. H. Jiang, X. Li, X. J. Zhang, Q. Ding, and T. Cai, "Morphology Control of Conjugated Microporous Polymer Networks for Visible-Light-Driven Oxidative Coupling of Amines," *Journal of Polymer Science* 62 (2023): 409–418, https://doi.org/10.1002/pol.20230755.

32. S. You, Z. Ding, R. Yuan, J. Long, and C. Xu, "Confined Synthesis of Conjugated Microporous Polymers for Selective Photocatalytic Oxidation of Amines," *Journal of Colloid & Interface Science* 664 (2024): 63–73, https://doi.org/10.1016/j.jcis.2024.03.031.

33. W.-K. An, S.-J. Zheng, Y.-N. Du, et al., "Thiophene-embedded Conjugated Microporous Polymers for Photocatalysis," *Catalysis Science & Technology* 10 (2020): 5171–5180, https://doi.org/10.1039/D0CY01164A.

34. R. Ren, Z. Jiao, Z. Li, Y. Tian, B. Liu, and G. Yue, "Polarization-Induced Proton Adsorption and Charge Separation in Pyrene-Based Conjugated Microporous Polymers via Substituent Regulation for Efficient Photocatalytic Hydrogen Evolution," *Journal of Catalysis* 421 (2023): 393–402, https://doi.org/10.1016/j.jcat.2023.03.038.

35. M. G. Mohamed, M. H. Elsayed, C.-J. Li, et al., "Reticular Design and Alkyne Bridge Engineering in Donor–π–Acceptor Type Conjugated Microporous Polymers for Boosting Photocatalytic Hydrogen Evolution," *Journal of Materials Chemistry A* 12 (2024): 7693–7710, https://doi.org/10.1039/D3TA07309B.

36. L. Chen, B. Chen, J. Kang, et al., "The Synthesis of a Novel Conjugated Microporous Polymer and Application on Photocatalytic Removal of Uranium(VI) From Wastewater Under Visible Light," *Chemical Engineering Journal* 431 (2022): 133222, https://doi.org/10.1016/j.cej.2021.133222.

37. L. Sun, Z. Liang, J. Yu, and R. Xu, "Luminescent Microporous Organic Polymers Containing the 1,3,5-Tri(4-Ethenylphenyl)Benzene Unit Constructed by Heck Coupling Reaction," *Polymer Chemistry* 4 (2013): 1932, https://doi.org/10.1039/c2py21034g.

38. N. Meng, H. Li, Y. Liu, and Y. Liao, "Self-Templating Synthesis of Nitrogen-Rich Porous Carbons Using Pyridyl Functionalized Conjugated Microporous Polytriphenylamine for Electrochemical Energy Storage," *Electrochimica Acta* 402 (2022): 139531, https://doi.org/10.1016/j.electacta.2021.139531.

39. H. Ma, F. Li, P. Li, et al., "A Dendrimer-Based Electropolymerized Microporous Film: Multifunctional, Reversible, and Highly Sensitive Fluorescent Probe," *Advanced Functional Materials* 26 (2016): 2025–2031, https://doi.org/10.1002/adfm.201504692.

40. H. Liu, Y. Wang, W. Mo, et al., "Dendrimer-Based, High-Luminescence Conjugated Microporous Polymer Films for Highly Sensitive and Selective Volatile Organic Compound Sensor Arrays," *Advanced Functional Materials* 30 (2020): 1910275, https://doi.org/10.1002/adfm.201910275.

41. W. Mo, Z. Zhu, F. Kong, et al., "Controllable Synthesis of Conjugated Microporous Polymer Films for Ultrasensitive Detection of Chemical Warfare Agents," *Nature Communications* 13 (2022): 5189, https://doi.org/10.1038/s41467-022-32878-w.

42. S. Li, H. Yu, Y. Wang, et al., "Exploring a Ni–N_4 Active Site-Based Conjugated Microporous Polymer Z-Scheme Heterojunction Through Covalent Bonding for Visible Light-Driven Photocatalytic CO_2 Conversion in Pure Water," *Small* 20 (2023): 2305900, https://doi.org/10.1002/smll.202305900.

43. L. Xiao, Q. Li, Y. Liu, et al., "Durable and Recyclable Conjugated Microporous Polymer Mediated Controlled Radical Polymerization Under White LED Light Irradiation," *Polymer Chemistry* 12 (2021): 6714–6723, https://doi.org/10.1039/D1PY01241J.

27662098, 2026, 2, Downloaded from https://onlinelibrary.wiley.com/doi/10.1002/EXP.20240487 by CochraneChina, Wiley Online Library on [08/06/2026]. See the Terms and Conditions (https://onlinelibrary.wiley.com/terms-and-conditions) on Wiley Online Library for rules of use; OA articles are governed by the applicable Creative Commons License

44. L. Zheng, Z. Lu, H. Yang, et al., "Electron Transport by Intramolecular Cascaded π-Conjugation Channels of D-A Two-Dimensional Conjugated Microporous Polymer Mediate Photo-Induced RCMP," *Polymer* 282 (2023): 126163, https://doi.org/10.1016/j.polymer.2023.126163.

45. S. Y. Yu, J. Mahmood, H. J. Noh, et al., "Direct Synthesis of a Covalent Triazine-Based Framework From Aromatic Amides," *Angewandte Chemie International Edition* 57 (2018): 8438–8442, https://doi.org/10.1002/anie.201801128.

46. J. Li, T. Chan, C. Jing, and J. Wang, "CO_2 photoreduction With High Selectivity of C_2H_4 Production on Conjugated Microporous Polymer With Cu Single Atoms," *Fuel* 357 (2024): 130020, https://doi.org/10.1016/j.fuel.2023.130020.

47. W. Wu, C. Feng, M. Chen, et al., "Novel Benzimidazole-Linked Microporous Conjugated Polymers for Highly Selective Adsorption and Photocatalytic Reduction of Diluted CO_2," *Green Chemistry* 25 (2023): 9335–9342, https://doi.org/10.1039/D3GC02966B.

48. Y. Liu, L. Yang, Y. Hou, et al., "2-Pyran-4-Ylidene Malononitrile Based Conjugated Microporous Polymers as Metal-Free Heterogeneous Photocatalysts for Organic Synthesis," *Macromolecular Rapid Communications* 45 (2024): 2400083, https://doi.org/10.1002/marc.202400083.

49. M. M. Samy, I. M. A. Mekhemer, M. G. Mohamed, et al., "Conjugated Microporous Polymers Incorporating Thiazolo[5,4-d]Thiazole Moieties for Sunlight-Driven Hydrogen Production From Water," *Chemical Engineering Journal* 446 (2022): 137158, https://doi.org/10.1016/j.cej.2022.137158.

50. B. Chen, N. Yang, P. Wang, Y. Xiang, and H. Chen, "Post-Side Chain Engineering of Difluorinated Benzothiadiazole-Based Conjugated Microporous Polymer for Enhanced Photocatalytic H_2 Evolution," *Applied Surface Science* 499 (2020), https://doi.org/10.1016/j.apsusc.2019.143865.

51. Z. Cheng, L. Wang, Y. He, et al., "Rapid Metal-Free Synthesis of Pyridyl-Functionalized Conjugated Microporous Polymers for Visible-Light-Driven Water Splitting," *Polymer Chemistry* 11 (2020): 3393–3397, https://doi.org/10.1039/D0PY00249F.

52. X. Gao, C. Shu, C. Zhang, et al., "Substituent Effect of Conjugated Microporous Polymers on the Photocatalytic Hydrogen Evolution Activity," *Journal of Materials Chemistry A* 8 (2020): 2404–2411, https://doi.org/10.1039/C9TA13212K.

53. W. Hao, R. Chen, Y. Zhang, Y. Wang, and Y. Zhao, "Triazine-Based Conjugated Microporous Polymers for Efficient Hydrogen Production," *ACS Omega* 6 (2021): 23782–23787, https://doi.org/10.1021/acsomega.1c02592.

54. C. Han, S. Xiang, M. Ge, P. Xie, C. Zhang, and J. X. Jiang, "An Efficient Electron Donor for Conjugated Microporous Polymer Photocatalysts With High Photocatalytic Hydrogen Evolution Activity," *Small* 18 (2022): 2202072, https://doi.org/10.1002/smll.202202072.

55. W.-J. Xiao, Y. Wang, W.-R. Wang, et al., "Diketopyrrolopyrrole-Based Donor–Acceptor Conjugated Microporous Polymers for Visible-Light-Driven Photocatalytic Hydrogen Production From Water," *Macromolecules* 53 (2020): 2454–2463, https://doi.org/10.1021/acs.macromol.9b02488.

56. Z. Cheng, Y. He, C. Yang, N. Meng, and Y. Liao, "Metal-Free Synthesis of Pyridyl Conjugated Microporous Polymers With Tunable Bandgaps for Efficient Visible-Light-Driven Hydrogen Evolution," *Chinese Chemical Letters* 34 (2023): 107440, https://doi.org/10.1016/j.cclet.2022.04.038.

57. A. F. Saber, A. M. Elewa, H.-H. Chou, and A. F. M. El-Mahdy, "Donor-Acceptor Carbazole-Based Conjugated Microporous Polymers as Photocatalysts for Visible-Light-Driven H_2 and O_2 Evolution From Water Splitting," *Applied Catalysis B: Environment and Energy* 316 (2022): 121624, https://doi.org/10.1016/j.apcatb.2022.121624.

58. L. Xu, C. Yang, Z. Cheng, et al., "Carbazole-Based Donor-Acceptor Conjugated Microporous Polymers for Efficient Visible-Light-Driven Photocatalytic H_2 Evolution," *Chinese Journal of Chemistry* 41 (2023): 2518–2524, https://doi.org/10.1002/cjoc.202300207.

59. T.-L. Lee, A. M. Elewa, M. G. Kotp, H.-H. Chou, and A. F. M. El-Mahdy, "Carbazole- and Thiophene-Containing Conjugated Microporous Polymers With Different Planarity for Enhanced Photocatalytic Hydrogen Evolution," *Chemical Communications* 57 (2021): 11968–11971, https://doi.org/10.1039/D1CC04551B.

60. Y. Wang, A. Vogel, M. Sachs, et al., "Current Understanding and Challenges of Solar-Driven Hydrogen Generation Using Polymeric Photocatalysts," *Nature Energy* 4 (2019): 746–760, https://doi.org/10.1038/s41560-019-0456-5.

61. C. Han, L. Hu, S. Jin, J. Ma, J.-X. Jiang, and C. Zhang, "Molecular Engineering in D-π-A-A-Type Conjugated Microporous Polymers for Boosting Photocatalytic Hydrogen Evolution," *ACS Applied Materials & Interfaces* 15 (2023): 36404–36411, https://doi.org/10.1021/acsami.3c07699.

62. C. Zhao, Z. Chen, R. Shi, X. Yang, and T. Zhang, "Active Site Engineering in Porous Electrocatalysts," *Advanced Materials* 32 (2020): 2002435.

63. C. Li, H. Xu, H. Xiong, et al., "Π-Bridge Modulations in D– π –A Conjugated Microporous Polymers to Facilitate Charge Separation and Transfer Kinetics for Efficient Photocatalysis," *Advanced Functional Materials* 34 (2024): 2405539, https://doi.org/10.1002/adfm.202405539.

64. C. Shu, C. Han, X. Yang, et al., "Boosting the Photocatalytic Hydrogen Evolution Activity for D–π–A Conjugated Microporous Polymers by Statistical Copolymerization," *Advanced Materials* 33 (2021): 2008498, https://doi.org/10.1002/adma.202008498.

65. C. Han, S. Xiang, S. Jin, C. Zhang, and J.-X. Jiang, "Rational Design of Conjugated Microporous Polymer Photocatalysts With Definite D–π–A Structures for Ultrahigh Photocatalytic Hydrogen Evolution Activity Under Natural Sunlight," *ACS Catal* 13 (2022): 204–212, https://doi.org/10.1021/acscatal.2c04993.

66. F. Li, X. Dai, L. Zhang, et al., "Triphenylamine Promoted Geometric Structure Adjusting of the Novel Macrocyclic Structure D-π-A Conjugated Microporous Polymers for Photocatalytic Hydrogen Evolution," *Fuel* 370 (2024): 131812, https://doi.org/10.1016/j.fuel.2024.131812.

67. X. Han, Y. Zhang, Y. Dong, J. Zhao, S. Ming, and J. Zhang, "Effect of the Cross-Linker Length of Thiophene Units on Photocatalytic Hydrogen Production of Triazine-Based Conjugated Microporous Polymers," *RSC Advances* 12 (2022): 708–718, https://doi.org/10.1039/D1RA07916F.

68. G. Zhang, A. M. Elewa, M. Rashad, S. Helali, H.-H. Chou, and A. F. M. El-Mahdy, "Triazine- and Porphyrin-Based Donor-Acceptor Microporous Conjugated Polymers for Enhanced Photocatalytic Hydrogen Production Activity," *Microporous and Mesoporous Materials* 363 (2024): 112824, https://doi.org/10.1016/j.micromeso.2023.112824.

69. G. Feng, Y. Sun, J. Yuan, et al., "A CMP-based [FeFe]-Hydrogenase Dual-Functional Biomimetic System for Photocatalytic Hydrogen Evolution Coupled With Degradation of Tetracycline," *Appl Catal B: Environ* 340 (2024): 123200, https://doi.org/10.1016/j.apcatb.2023.123200.

70. S. U. Sharma, M. H. Elsayed, I. M. A. Mekhemer, et al., "Rational Design of Pyrene and Thienyltriazine-Based Conjugated Microporous Polymers for High-Performance Energy Storage and Visible-Light Photocatalytic Hydrogen Evolution From Water," *Giant* 17 (2024): 100217, https://doi.org/10.1016/j.giant.2023.100217.

71. A. Naldoni, M. Altomare, G. Zoppellaro, et al., "Photocatalysis With Reduced TiO_2: From Black TiO_2 to Cocatalyst-Free Hydrogen Production," *ACS Catalysis* 9 (2018): 345–364, https://doi.org/10.1021/acscatal.8b04068.

72. Y. Liu, J. Quiñonero, L. Yao, et al., "Defect Engineered Nanostructured $LaFeO_3$ Photoanodes for Improved Activity in Solar Water Oxidation," *Journal of Materials Chemistry A* 9 (2021): 2888–2898, https://doi.org/10.1039/D0TA11541J.

73. Y. Liu, A. Bin Mohamad Annuar, S. Rodriguez-Jimenez, et al., "Solar Fuel Synthesis Using a Semiartificial Colloidal Z-Scheme," *Journal of the American Chemical Society* 146 (2024): 29865–29876, https://doi.org/10.1021/jacs.4c11827.

27662098, 2026, 2, Downloaded from https://onlinelibrary.wiley.com/doi/10.1002/EXP.20240487 by CochraneChina, Wiley Online Library on [08/06/2026]. See the Terms and Conditions (https://onlinelibrary.wiley.com/terms-and-conditions) on Wiley Online Library for rules of use; OA articles are governed by the applicable Creative Commons License

74. Q. Guo, Z. Ma, C. Zhou, Z. Ren, and X. Yang, "Single Molecule Photocatalysis on TiO_2 Surfaces," *Chemical Reviews* 119 (2019): 11020–11041, https://doi.org/10.1021/acs.chemrev.9b00226.

75. Q. Sun, N. Wang, J. Yu, and J. C. Yu, "A Hollow Porous CdS Photocatalyst," *Advanced Materials* 30, no. 45 (2018): 1804368.

76. S. Barman, A. Singh, F. A. Rahimi, and T. K. Maji, "Metal-Free Catalysis: A Redox-Active Donor–Acceptor Conjugated Microporous Polymer for Selective Visible-Light-Driven CO_2 Reduction to CH_4," *Journal of the American Chemical Society* 143 (2021): 16284–16292, https://doi.org/10.1021/jacs.1c07916.

77. W. Wu, C. Dai, M. Wu, Y. Chen, C. Zeng, and F. Li, "Red-Light-Driven CO_2 Photoreduction Into CH_4 and CO Enabled by Narrow-Gap Conjugated Microporous Polymers," *Solar RRL* 7 (2022): 2200907, https://doi.org/10.1002/solr.202200907.

78. W. Zhao, D. Zhai, C. Liu, et al., "Unblocked Intramolecular Charge Transfer for Enhanced CO_2 Photoreduction Enabled by an Imidazolium-Based Ionic Conjugated Microporous Polymer," *Applied Catalysis B: Environment and Energy* 300 (2022): 120719, https://doi.org/10.1016/j.apcatb.2021.120719.

79. F. A. Rahimi, S. Dey, P. Verma, and T. K. Maji, "Photocatalytic CO_2 Reduction Based on a Re(I)-Integrated Conjugated Microporous Polymer: Role of a Sacrificial Electron Donor in Product Selectivity and Efficiency," *ACS Catalysis* 13 (2023): 5969–5978, https://doi.org/10.1021/acscatal.3c00053.

80. F. Meng, J. Wang, M. Chen, Z. Wang, G. Bai, and X. Lan, "Extending the π-Conjugated System in Conjugated Microporous Polymers to Modulate Excitonic Effects for Metal-Free Selective CO_2 Photoreduction to CH_4," *ACS Catalysis* 13 (2023): 12142–12152, https://doi.org/10.1021/acscatal.3c02950.

81. B. Chen, L. Chen, Z. Yan, et al., "Conjugated Microporous Polymers as a Visible Light Driven Platform for Photo-Redox Conversion of Biomass Derived Chemicals," *Green Chemistry* 23 (2021): 3607–3611, https://doi.org/10.1039/D1GC00762A.

82. Y. Yan, X. Yu, C. Shao, Y. Hu, W. Huang, and Y. Li, "Atomistic Structural Engineering of Conjugated Microporous Polymers Promotes Photocatalytic Biomass Valorization," *Advanced Functional Materials* 33 (2023): 2304604, https://doi.org/10.1002/adfm.202304604.

83. H. Zang, K. Wang, M. Zhang, R. Xie, L. Wang, and E. Y. X. Chen, "Catalytic Coupling of Biomass-Derived Aldehydes Into Intermediates for Biofuels and Materials," *Catalysis Science & Technology* 8 (2018): 1777–1798, https://doi.org/10.1039/C7CY02221B.

84. S. C. Y. Wu, J. Wu, F. Liu, et al., "Revivable Self-Assembled Supramolecular Biomass Fibrous Framework for Efficient Microplastic Removal," *Science Advances* 10 (2024): eadn8662, https://doi.org/10.1126/sciadv.adn8662.

85. Y. Wu, C. Ye, F. Liu, et al., "Highly Efficient, Recyclable Microplastic Adsorption Enabled by Chitin Hydrogen Bond Network Rearrangement," *Advanced Functional Materials* 34 (2024): 2311075, https://doi.org/10.1002/adfm.202311075.

86. C. Xu, E. Paone, D. Rodríguez-Padrón, R. Luque, and F. Mauriello, "Recent Catalytic Routes for the Preparation and the Upgrading of Biomass Derived Furfural and 5-Hydroxymethylfurfural," *Chemical Society Reviews* 49 (2020): 4273–4306, https://doi.org/10.1039/D0CS00041H.

87. N. Corrigan, K. Jung, G. Moad, C. J. Hawker, K. Matyjaszewski, and C. Boyer, "Reversible-Deactivation Radical Polymerization (Controlled/Living Radical Polymerization): From Discovery to Materials Design and Applications," *Progress in Polymer Science* 111 (2020): 101311, https://doi.org/10.1016/j.progpolymsci.2020.101311.

88. A. M. Doerr, J. M. Burroughs, S. R. Gitter, X. Yang, A. J. Boydston, and B. K. Long, "Advances in Polymerizations Modulated by External Stimuli," *ACS Catal* 10 (2020): 14457–14515, https://doi.org/10.1021/acscatal.0c03802.

89. S. Dadashi-Silab, F. Lorandi, M. J. DiTucci, et al., "Conjugated Cross-Linked Phenothiazines as Green or Red Light Heterogeneous Photocatalysts for Copper-Catalyzed Atom Transfer Radical Polymerization," *Journal of the American Chemical Society* 143 (2021): 9630–9638, https://doi.org/10.1021/jacs.1c04428.

90. X. Li, X. J. Zhang, W. L. Guo, Y. Huang, and T. Cai, "Shape-Controlled Synthesis of Conjugated Microporous Polymer Nanotubes and Their Implementation in Continuous Flow Polymerization," *Chemical Engineering Journal* 465 (2023): 142861, https://doi.org/10.1016/j.cej.2023.142861.

91. Y. Huang, Q. Xiang, X. Li, and T. Cai, "Enhancing Aqueous Reversible Addition–Fragmentation Chain Transfer Photopolymerization in Continuous Flow Reactors With Hairy Hollow Conjugated Microporous Polymer Nanocomposites," *Macromolecules* 57 (2024): 5081–5091, https://doi.org/10.1021/acs.macromol.4c00736.

92. F. Yu, Z. Zhu, C. Li, et al., "A Redox-Active Perylene-Anthraquinone Donor-Acceptor Conjugated Microporous Polymer With an Unusual Electron Delocalization Channel for Photocatalytic Reduction of Uranium (VI) in Strongly Acidic Solution," *Applied Catalysis B: Environment and Energy* 314 (2022): 121467, https://doi.org/10.1016/j.apcatb.2022.121467.

93. X. Cao, Z. Lu, H. Yang, R. Zhao, L. Xiao, and L. Hou, "Visible Light-Triggered Non-Deoxygenated PET–RAFT Polymerization by Heterogeneous Conjugated Microporous Polymer Photocatalysts," *Polymer Chemistry* 15 (2024): 1504–1510, https://doi.org/10.1039/D4PY00243A.

94. J. Chakraborty, I. Nath, C. Jabbour, et al., "Novel Rapid Room Temperature Synthesis of Conjugated Microporous Polymer for Metal-Free Photocatalytic Degradation of Fluoroquinolones," *Journal of Hazardous Materials* 398 (2020): 122928, https://doi.org/10.1016/j.jhazmat.2020.122928.

95. X. Cui, Y. Li, W. Dong, D. Liu, and Q. Duan, "Microwave-Assisted Synthesis of Novel Imine-Linked Copper Porphyrin Conjugated Microporous Polymers as Heterogeneous Photocatalysts," *Reactive & Functional Polymers* 154 (2020): 104633, https://doi.org/10.1016/j.reactfunctpolym.2020.104633.

96. A. Liu, L. Chen, L. Qi, et al., "Biosafe, Rapid, and Ultrahigh-Capacity Endotoxin Purification in Blood by a Sustainable and Recyclable MOF-Functionalized Chitin Microsphere Adsorbent," *SusMat* 4 (2024): e235, https://doi.org/10.1002/sus2.235.

97. B. Chen, G. Zhang, L. Chen, et al., "Visible Light Driven Photocatalytic Removal of Uranium(VI) in Strongly Acidic Solution," *Journal of Hazardous Materials* 426 (2022): 127851, https://doi.org/10.1016/j.jhazmat.2021.127851.

98. A. F. Saber, C. C. Chueh, M. Rashad, S. W. Kuo, and A. F. M. El-Mahdy, "Thiazolyl-Linked Conjugated Microporous Polymers for Enhancement Adsorption and Photocatalytic Degradation of Organic Dyes From Water," *Mater Today Sustainability* 23 (2023): 100429, https://doi.org/10.1016/j.mtsust.2023.100429.

99. M. G. Kotp, C.-L. Chang, and A. F. M. El-Mahdy, "Tetraphenyl-p-Phenylenediamine-Based Tunable Conjugated Microporous Polymers: Adsorption and Photodegradation of Hazardous Dyestuff in Aqueous Environments," *Journal of Water Process Engineering* 53 (2023): 103675, https://doi.org/10.1016/j.jwpe.2023.103675.

100. J. Yu, Q.-M. Hasi, Y. Guo, et al., "Porphyrin-Based Conjugated Microporous Polymer Loaded With Nanoscale Zerovalent Iron for the Degradation of Organic Pollutants Under Visible Light," *Langmuir* 40 (2024): 4739–4750, https://doi.org/10.1021/acs.langmuir.3c03507.

101. Y. Li, M. Liu, and L. Chen, "Polyoxometalate Built-In Conjugated Microporous Polymers for Visible-Light Heterogeneous Photocatalysis," *Journal of Materials Chemistry A* 5 (2017): 13757–13762, https://doi.org/10.1039/C7TA03776G.

102. W. Zhao, C. Yang, J. Huang, et al., "Selective Aerobic Oxidation of Sulfides to Sulfoxides in Water Under Blue Light Irradiation Over

27662098, 2026, 2, Downloaded from https://onlinelibrary.wiley.com/doi/10.1002/EXP.20240487 by CochraneChina, Wiley Online Library on [08/06/2026]. See the Terms and Conditions (https://onlinelibrary.wiley.com/terms-and-conditions) on Wiley Online Library for rules of use; OA articles are governed by the applicable Creative Commons License

$Bi_4O_5Br_2$," *Green Chemistry* 22 (2020): 4884–4889, https://doi.org/10.1039/D0GC01930E.

103. X. Li, X. Ma, F. Zhang, X. Dong, and X. Lang, "Selective Photocatalytic Formation of Sulfoxides by Aerobic Oxidation of Sulfides Over Conjugated Microporous Polymers With Thiazolo[5,4-d]Thiazole Linkage," *Appl Catal B: Environ* 298 (2021): 120514, https://doi.org/10.1016/j.apcatb.2021.120514.

104. Y. Wang, X. Li, X. Dong, F. Zhang, and X. Lang, "Triazine-Based Two Dimensional Porous Materials for Visible Light-Mediated Oxidation of Sulfides to Sulfoxides With O_2," *Journal of Colloid & Interface Science* 616 (2022): 846–857, https://doi.org/10.1016/j.jcis.2022.02.114.

105. X. Li, Y. Wang, F. Zhang, and X. Lang, "Symmetry-Dependent Photocatalysis of Conjugated Microporous Polymers Based on Pyrene for Oxygenation of Sulfides With O_2," *Appl Catal B: Environ* 340 (2024): 123190, https://doi.org/10.1016/j.apcatb.2023.123190.

106. F. Huang, Y. Wang, K. Zhang, and X. Lang, "Benzotrithiophene Conjugated Microporous Polymer Photocatalysts for Selective Aerobic Sulfoxidation Driven by Green Light," *Catalysis Today* 434 (2024): 114671, https://doi.org/10.1016/j.cattod.2024.114671.

107. W. Sun, Y. Xiang, Z. Jiang, et al., "Designed Polymeric Conjugation Motivates Tunable Activation of Molecular Oxygen in Heterogeneous Organic Photosynthesis," *Science Bulletin* 67 (2022): 61–70, https://doi.org/10.1016/j.scib.2021.07.016.

108. Y. Z. Peng, G. C. Guo, S. Guo, L. H. Kong, T. B. Lu, and Z. M. Zhang, "Charge Transfer From Donor to Acceptor in Conjugated Microporous Polymer for Enhanced Photosensitization," *Angewandte Chemie, International Edition* 60 (2021): 22062–22069, https://doi.org/10.1002/anie.202109968.

109. X. Dong, H. Hao, F. Zhang, and X. Lang, "Combining Brønsted Base and Photocatalysis Into Conjugated Microporous Polymers: Visible Light-Induced Oxidation of Thiols Into Disulfides With Oxygen," *Journal of Colloid & Interface Science* 622 (2022): 1045–1053, https://doi.org/10.1016/j.jcis.2022.04.162.

110. R. Chen, J. L. Shi, Y. Ma, G. Lin, X. Lang, and C. Wang, "Designed Synthesis of a 2D Porphyrin-Based sp 2 Carbon-Conjugated Covalent Organic Framework for Heterogeneous Photocatalysis," *Angewandte Chemie, International Edition* 58 (2019): 6430–6434, https://doi.org/10.1002/anie.201902543.

111. J. Wen, X. Yang, Z. Sun, et al., "Biomimetic Photocatalytic Sulfonation of Alkenes to Access β-Ketosulfones With Single-Atom Iron Site," *Green Chemistry* 22 (2020): 230–237, https://doi.org/10.1039/C9GC03580J.

112. Y. Wang, W. Zhang, Y. Yang, et al., "Visible-Light-Driven Cr(VI) Reduction by Ferrocene-Integrated Conjugated Porous Polymers via Dual Catalytic Routes," *Chemical Communications* 57 (2021): 4886–4889, https://doi.org/10.1039/D1CC01079D.

113. Z. Li, H. Song, R. Guo, et al., "Visible-Light-Induced Condensation Cyclization to Synthesize Benzimidazoles Using Fluorescein as a Photocatalyst," *Green Chemistry* 21 (2019): 3602–3605, https://doi.org/10.1039/C9GC01359H.

114. C. T. J. Ferguson, N. Huber, T. Kuckhoff, K. A. I. Zhang, and K. Landfester, "Dispersible Porous Classical Polymer Photocatalysts for Visible Light-Mediated Production of Pharmaceutically Relevant Compounds in Multiple Solvents," *Journal of Materials Chemistry A* 8 (2020): 1072–1076, https://doi.org/10.1039/C9TA11242A.

115. S. Han, Z. Li, S. Ma, et al., "Bandgap Engineering in Benzotrithiophene-Based Conjugated Microporous Polymers: A Strategy for Screening Metal-Free Heterogeneous Photocatalysts," *Journal of Materials Chemistry A* 9 (2021): 3333–3340, https://doi.org/10.1039/D0TA10232F.

116. L. Liu, K. Dong, M. Hassan, W. Gong, J. Cui, and G. Ning, "Incorporation of Carbazole and Boron-Containing Dye Into Conjugated Microporous Polymers With Significant Aerobic Oxidative Photocatalysis," *Green Synthesis and Catalysis* 3 (2022): 349–356.

117. S. Li, J. Yin, H. Zhang, and K. A. I. Zhang, "Dual Molecular Oxygen Activation Sites on Conjugated Microporous Polymers for Enhanced Photocatalytic Formation of Benzothiazoles," *ACS Applied Materials & Interfaces* 15 (2023): 2825–2831, https://doi.org/10.1021/acsami.2c16581.

118. S. Li, W. Zhang, S. Yang, et al., "Phenothiazine-Based Conjugated Microporous Polymers: Pore Surface and Bandgap Engineering for Visible Light-Driven Aerobic Oxidative Cyanation," *Chemical Engineering Journal* 408 (2021): 127261, https://doi.org/10.1016/j.cej.2020.127261.

119. X. Dong, Y. Wang, F. Huang, and X. Lang, "Carbazole–Anthraquinone Conjugated Microporous Polymer Photocatalysis for Aerobic Oxidative Cyanation of Tertiary Amines Irradiated by Green Light," *Chemical Engineering Journal* 469 (2023): 143934, https://doi.org/10.1016/j.cej.2023.143934.

120. X. Dong, H. Hao, F. Zhang, and X. Lang, "Blue Light Photocatalysis of Carbazole-based Conjugated Microporous Polymers: Aerobic Hydroxylation of Phenylboronic Acids to Phenols," *Applied Catalysis B: Environment and Energy* 309 (2022): 121210, https://doi.org/10.1016/j.apcatb.2022.121210.

121. S. Sau and S. K. Samanta, "Triphenylamine–Anthraquinone Based Donor–Acceptor Conjugated Microporous Polymers for Photocatalytic Hydroxylation of Phenylboronic Acids," *Chemical Communications* 59 (2023): 635–638, https://doi.org/10.1039/D2CC05334A.

122. R. S. Keri, M. R. Patil, S. A. Patil, and S. Budagumpi, "A Comprehensive Review in Current Developments of Benzothiazole-Based Molecules in Medicinal Chemistry," *European Journal of Medicinal Chemistry* 89 (2015): 207–251, https://doi.org/10.1016/j.ejmech.2014.10.059.

123. C.-A. Wang, J.-P. Zhang, K. Nie, et al., "Tetrathienoanthracene-Functionalized Conjugated Microporous Polymers as an Efficient, Metal-Free Visible-Light Solid Organocatalyst for Heterogeneous Photocatalysis," *Catalysis Science & Technology* 11 (2021): 3799–3809, https://doi.org/10.1039/D1CY00488C.

124. J. Jiang, Z. Liang, X. Xiong, X. Zhou, and H. Ji, "A Carbazolyl Porphyrin-Based Conjugated Microporous Polymer for Metal-Free Photocatalytic Aerobic Oxidation Reactions," *Chemcatchem* 12 (2020): 3523–3529, https://doi.org/10.1002/cctc.202000199.

125. H. Xu, X. Li, H. Hao, X. Dong, W. Sheng, and X. Lang, "Designing Fluorene-Based Conjugated Microporous Polymers for Blue Light-Driven Photocatalytic Selective Oxidation of Amines With Oxygen," *Applied Catalysis B: Environment and Energy* 285 (2021): 119796, https://doi.org/10.1016/j.apcatb.2020.119796.

126. W. Gong, X. Deng, K. Dong, L. Liu, and G. Ning, "A Boranil-Based Conjugated Microporous Polymer for Efficient Visible-Light-Driven Heterogeneous Photocatalysis," *Polymer Chemistry* 12 (2021): 3153–3159, https://doi.org/10.1039/D1PY00297J.

127. X. Dong, F. Zhang, F. Huang, and X. Lang, "Pyrene-Based Conjugated Microporous Polymers for Red Light-Powered Oxidation of Amines to Imines," *Applied Catalysis B: Environment and Energy* 318 (2022): 121875, https://doi.org/10.1016/j.apcatb.2022.121875.

128. F. Huang, X. Dong, Y. Wang, and X. Lang, "Narrowing the Bandgaps of Thiazolo[5,4-d]Thiazole-bridged Conjugated Microporous Polymers to Capture Green Light for Selective Oxidation of Amines," *Applied Catalysis B: Environment and Energy* 330 (2023): 122585, https://doi.org/10.1016/j.apcatb.2023.122585.

129. X. Li, F. Zhang, Y. Wang, K. Xiong, and X. Lang, "Extending the 2D Conjugated Microporous Polymers Linked by Thiazolo[5,4-d]Thiazole for Green Light-Driven Selective Aerobic Oxidation of Amines," *Journal of Materials Chemistry A* 10 (2022): 14965–14975, https://doi.org/10.1039/D2TA02603A.

130. K. Zhang, X. Dong, B. Zeng, K. Xiong, and X. Lang, "Red Light Photocatalysis of Conjugated Microporous Polymers Based on Fused Thiophenes for Selective Oxidation of Amines," *Journal of Colloid & Interface Science* 651 (2023): 622–632, https://doi.org/10.1016/j.jcis.2023.08.003.

27662098, 2026, 2, Downloaded from https://onlinelibrary.wiley.com/doi/10.1002/EXP.20240487 by CochraneChina, Wiley Online Library on [08/06/2026]. See the Terms and Conditions (https://onlinelibrary.wiley.com/terms-and-conditions) on Wiley Online Library for rules of use; OA articles are governed by the applicable Creative Commons License

131. Q. Xiang, Y. Huang, S. H. Jiang, S. X. Cheng, X. Li, and T. Cai, "Utilizing Hairy Hollow Conjugated Microporous Polymers and Native Enzymes for Precise Aerobic Photocatalysis Under Near-Infrared Wavelengths," *Advanced Functional Materials* 34, no. 29 (2024): 2400512, https://doi.org/10.1002/adfm.202400512.

132. G. Wei, L. Wang, Z. Ding, R. Yuan, J. Long, and C. Xu, "Carbazole-Involved Conjugated Microporous Polymer Hollow Spheres for Selective Photocatalytic Oxidation of Benzyl Alcohol Under Visible-Light Irradiation," *Journal of Colloid & Interface Science* 642 (2023): 648–657, https://doi.org/10.1016/j.jcis.2023.03.196.

133. W. Zhang, D. Wang, Q. Xie, et al., "Enhanced Reducibility via Altering Exciton Binding Energy of Conjugated Microporous Polymers for Photocatalytic Reduction," *Macromolecules* 56 (2023): 4022–4029, https://doi.org/10.1021/acs.macromol.3c00241.

27662098, 2026, 2, Downloaded from https://onlinelibrary.wiley.com/doi/10.1002/EXP.20240487 by CochraneChina, Wiley Online Library on [08/06/2026]. See the Terms and Conditions (https://onlinelibrary.wiley.com/terms-and-conditions) on Wiley Online Library for rules of use; OA articles are governed by the applicable Creative Commons License